

# HOW SOCIAL INTERACTIONS MATTER WHEN DISTANCE DIES?\*

Minoru Osawa<sup>†</sup>      José M. Gaspar<sup>‡</sup>

May 28, 2022

## Abstract

We consider an economic geography model with two inter-regional proximity structures, one due to trade linkages and the other due to social interactions. We investigate how the network structure of social interactions, or the social proximity structure, affects the timing of endogenous agglomeration and the spatial distribution of workers across regions. Endogenous agglomeration emerges when inter-regional trade and/or social interactions incur high transportation costs, and the uniform dispersion occurs when these costs become negligibly small (i.e., when distance dies). In many-region geography, the network structure of social proximity emerges as the determinant of the geographical distribution of workers when trade becomes freer. If social proximity is governed by geographical distance (as in ground transportation), a mono-centric concentration emerges. If geographically distant pairs of regions are “socially close” (due to, e.g., passenger transportation modes with strong distance economy such as regional airlines), then geographically multi-centric spatial distribution can be sustainable.

**Keywords:** social network; agglomeration; dispersion; many regions; stability.

**JEL Classification:** C62, R12, R13, R14

---

\*We wish to thank Shota Fujishima and Yuki Takayama for insightful comments. Minoru Osawa thank grant support from JSPS Kakenhi 17H00987 and 19K15108. José M. Gaspar gratefully acknowledges financial support from Fundação para a Ciência e Tecnologia (through projects UID/GES/00731/2019, PTDC/EGE-ECO/30080/2017 and CEECIND/02741/2017).

<sup>†</sup>Corresponding author: minoru.osawa.a5@tohoku.ac.jp / osawa.minoru@gmail.com, Tohoku University

<sup>‡</sup>jgaspar@porto.ucp.pt, CECE and Católica Porto Business School, Universidade Católica Portuguesa

# 1 Introduction

The spectacular drop in transportation costs ever since the Industrial Revolution has led to the concentration of economic activities and population to fewer and fewer geographical locations. Spatial economic theory has emphasized the roles of endogenous forces, hitherto outweighed by first-order exogenous heterogeneities of locations, in shaping the lasting and sizable economic agglomerations. Such localization of production in a small number of selected locations is currently in the process of evening out, partly due to the far-reaching developments in information and communication technologies that have made it possible to organize complex production processes even when they were separated by geographical distance (Baldwin, 2016). Hand-in-hand with the shift of values towards service-oriented and high-tech sectors, the economic geography in matured economies in the current era is shaped more and more by interactions between people.

This paper addresses how interactions between people affect the unbundling process of a geographically mono-centric economic agglomeration when inter-regional trade costs and/or communication costs become negligibly small (i.e., when distance dies). To obtain first-order theoretical implications, we develop a bare-bones economic geography model with one differentiated sector and a finite number of locations. Trade of goods is costly. There is inter-regional productivity spillover through social interactions. With the model, we draw qualitative insights into the role of interactions between people on the *timing* and the *form* of workers' agglomeration and dispersion across regions.

We build on the general equilibrium framework proposed by Allen and Arkolakis (2014); we assume a perfectly competitive Armington model with positive externalities and iceberg transportation costs. The key difference is that we assume that the productivity of a region depends on the whole spatial distribution of workers, in contrast to local spillover within each region. As Rosenthal and Strange (2019) shows, agglomeration effects act in various spatial scales — e.g., the regional, metropolitan, and neighborhood scales, or even within each building. To represent such effects in a flexible fashion, we assume that a region's productivity depends on an *social proximity matrix*  $\mathbf{G} = [\psi_{ij}]$  that represents the structure of inter-regional communication between people. Each  $\psi_{ij} \in (0, 1]$  represents the level of positive externality a worker in region  $j$  has on one in region  $i$ , so that region  $i$ 's productivity is given by  $a_i = \sum_j \psi_{ij} x_j$  where  $x_j$  denotes the mass of workers in region  $j$ . This setup includes, as a special case, spatially decaying technological externalities in urban models if, e.g.,  $\psi_{ij} = \exp(-\tau \ell_{ij})$  with  $\tau > 0$  and geographical distance  $\ell_{ij}$  between locations  $i$  and  $j$  (e.g., Fujita and Ogawa, 1982; Ahlfeldt et al., 2015). By considering the general specification, we can disentangle the role played by the underlying geographical proximity structure and that played by social interactions between people.

We first consider a symmetric two-region economy to elucidate the basic workings of the social interactions. There are two key transportation cost parameters: the freeness of trade and that of social interactions. Endogenous agglomeration emerges when the freeness of trade between regions and/or the freeness of social interactions between regions are low. The symmetric dispersion of workers occurs when trade and social interactions become free, i.e., when distance dies. When transportation is prohibitly costly, there is a full agglomeration of workers in one of the regions. As transportation costs decline, this asymmetry is gradually resolved; the spatial

configuration become increasingly symmetric, leading to the symmetric dispersion at threshold values of transportation costs. This behavior is akin to the dispersion process in economic geography models with urban costs (e.g., [Helpman, 1998](#); [Tabuchi, 1998](#)) in that dispersion occur when trade is freer, although our model do not have urban costs. The role of the additional dimension — social interactions — is also intuitive. When social interactions are less costly, dispersion is selected because there is fewer incentive to form agglomeration (i.e., the “death of distance”).

We then explore a symmetric four-region economy and consider various structure for social proximity. It is the minimal setting to investigate the roles of the *network structure* of  $\mathbf{G}$ , since non-trivial (but symmetric) network structures can emerge only when the number of regions is greater than three. Similar to the two-region setup, one of the regions attracts almost all workers when trade and social interaction costs are very high. The economy exhibits a gradual dispersion when these costs go down. The agglomeration force tends to support geographically mono-centric pattern of workers along the dispersion process. If the social proximity structure is more integrated as a whole, then agglomeration is less likely compared with less integrated networks. This is because endogenous advantage due to social proximity plays less prominent role when the economy is socially more integrated. Also, if some pair of regions are “socially closer,” then various geographical configurations other than the mono-centric pattern can be sustainable. For instance, geographically duo-centric concentration of workers emerges if geographically distant pairs of regions are socially close because of, e.g., passenger transportation modes with strong distance economy (such as regional airlines). In sum, the *network structure* of social interactions can govern when the dispersion is attained and how it looks like in the process of unbundling of a mono-centric economic agglomeration.

Out for simplicity and clarity, we build on a compromise that social proximity matrix  $\mathbf{G}$  is exogenously given. There are various possible micro-foundations for  $\mathbf{G}$ . For instance, it may represent the roles played by *passenger travels* that supports face-to-face contacts. It may be some aggregate measure, embedded in regional space, of the inter-*individual* social network that support information exchange and diffusion between regions. It can also be a reduced-form for the decision of *big players* such as large companies which open up branches in provincial cities, or airline companies connecting major regional cities. All of the interpretations above are meant to be described by sophisticated models, so that the structure of  $\mathbf{G}$  may be endogenously determined by micro-economic mechanisms. We instead give  $\mathbf{G}$  exogenously, for our aim in this paper is to provide the first-order insights into the workings of an additional inter-regional linkage other than goods trade. This strategy is akin to that in the network game literature ([Jackson, 2010](#)) that focuses on the roles of the structure of the inter-individual social network, or to that in the economic geography literature in general where it is a standard approach to suppose an exogenous inter-regional proximity structure.

In the following, Section 2 discusses related literature. Section 3 formulates the model. Section 4 studies the model in the simplest possible setup, the symmetric two-region economy. Section 5 illustrates the fundamental roles of the structure of the interaction network  $\mathbf{G}$ . In this section, we follow the strategy taken by [Matsuyama \(2017\)](#), in that we illustrate the effects of variation in the inter-regional proximity structure  $\mathbf{G}$  employing stylized examples. Section 6 concludes the paper.

## 2 Related literature

The current unbundling process of economic agglomeration may also be explained by the “bell-shaped development” narrative for industrial agglomeration (Fujita and Thisse, 2013, Section 8). The seminal theory of endogenous regional agglomeration after Krugman (1991) predicts that the spatial distribution of economic activities in a country is organized into a mono-centric state as transportation costs decline below a certain threshold in a many-region economy (Tabuchi and Thisse, 2011; Ikeda et al., 2012; Akamatsu et al., 2012, 2019). This prediction is qualitatively consistent with data (Tabuchi, 2014). A further decline of inter-regional transportation cost induces the flattening of mono-centric agglomeration (Helpman, 1998; Tabuchi, 1998), due to the rise of the relative importance of urban costs, e.g., higher land rent and commuting costs. There is ample evidence for the decline of peak population or production level of cities when transportation access improves (e.g., Baum-Snow, 2007; Baum-Snow et al., 2017). We may thus interpret that developed economies now face this final stage where once established economic clusters dissolve. These theories, however, do not address how interactions between people matter for regional economy because they deliberately focused on trade linkages as *the* mode of inter-location interaction in favor of tractability (Fujita and Mori, 2005). Given the importance of people’s communication in more and more information-intensive economies, we need a tractable theory that integrates social interactions into general equilibrium economic geography models. This paper is one of such attempts.

The interesting literature of inter-individual social interactions and cities (e.g., Helsley and Zenou, 2014; Picard and Zenou, 2018) is thus related to our study. Also, the important literature on economics of agglomeration (e.g., Beckmann, 1976; Fujita and Ogawa, 1982; Lucas and Rossi-Hansberg, 2002; Helsley and Strange, 2014) examines how inter-location externalities influence the urban spatial structure including the location of firms and households (see Fujita and Thisse, 2013, for a survey). We take an intermediate strategy between the former emerging literature, which focuses on individual-level social interactions, and the latter literature, which focuses on geographical proximity as the determinant of agglomeration economy. All the above models are different from ours since we consider regional scale.

A question then arises about how inter-regional spillover can arise. Even though various micro-foundations can be considered (as briefly discussed in the introduction), we highlight the role of knowledge creation due to interaction between *different cultures*. According to Fujita (2007), geography is an essential feature of knowledge creation and diffusion. For instance, people residing in the same region interact more frequently and thus contribute to develop the same, regional set of cultural ideas. Since geographically distant regions tend to develop different cultures, the economy as a whole evolves according to the synergy which results from *interactions across different regions* (i.e., different cultures). That is, as emphasized by Duranton and Puga (2001), knowledge creation and location are inter-dependent. Berliant and Fujita (2012) developed a model of spatial knowledge interactions and showed that higher cultural diversity and costly communication promote the productivity of knowledge creation, which corroborates the empirical findings of Ottaviano and Peri (2006, 2008) as well as the theoretical model of Ottaviano and Prarolo (2009). If interaction between different regions with different cultures promotes knowledge

creation, a region with good access in *passenger transport* will be more innovative and productive. Our flexible model integrates such effects into a general equilibrium framework with costly trade.

Technically, we build on a general analytical method for an economic geography model developed in Ikeda et al. (2012) and Akamatsu et al. (2012), which is recently synthesized in Akamatsu et al. (2019). Also, our four-region analysis is inspired by Matsuyama (2017), who considers various tractable geographical settings to investigate how the underlying geographical structure affects the home-market effect in multi-region economy. Barbero and Zoffio (2016) is also related to ours, for they focus on the role played by the topology of the underlying transportation network.

### 3 The Model

Consider an economy comprised of  $n$  regions, and let  $\mathcal{N} \equiv \{1, 2, \dots, n\}$  denote the set of regions. The economy is inhabited by a unit mass continuum of workers who are freely mobile across regions. Each worker chooses one of the regions to locate in. The spatial distribution of workers is denoted by  $\mathbf{x} = (x_i)_{i \in \mathcal{N}}$ , where  $x_i \geq 0$  is the mass of workers in region  $i \in \mathcal{N}$ . The set of all possible  $\mathbf{x}$  is therefore  $(n - 1)$ -dimensional simplex  $\mathcal{X} \equiv \{\mathbf{x} \geq \mathbf{0} \mid \sum_{i \in \mathcal{N}} x_i = 1\}$ .

We take the Armington (1969) assumption. Each region produces a distinct variety of the horizontally differentiated good. Workers derive utility from the consumption of differentiated varieties. The workers are homogeneous and have identical constant-elasticity-of-substitution (CES) preferences over differentiated varieties. Because the utility function is homothetic, the total welfare in region  $j \in \mathcal{N}$  is

$$U_j = \left( \sum_{i \in \mathcal{N}} q_{ij}^{\frac{\sigma-1}{\sigma}} \right)^{\frac{\sigma}{\sigma-1}}, \quad (3.1)$$

where  $\sigma > 1$  is the elasticity of substitution between varieties and  $q_{ij}$  is the amount of good produced in region  $i$  and consumed in region  $j$ .

Production is perfectly competitive and labor is the only input factor. Each worker provides a unit of labor inelastically in the region where they live and is compensated with a wage. The nominal market wage in region  $j \in \mathcal{N}$  is denoted by  $w_j \geq 0$ , and its spatial pattern by  $\mathbf{w} = (w_i)_{i \in \mathcal{N}}$ . The wage is determined in market equilibrium which we describe later.

The only (external) centripetal force in the model comes from social interactions. We assume that the productivity in region  $i$  is given as:

$$a_i(\mathbf{x}) = \sum_{j \in \mathcal{N}} \psi_{ij} x_j, \quad (3.2)$$

where  $\psi_{ij}$  is the level of externalities from  $j$  to  $i$ . We denote  $\mathbf{G} \equiv [\psi_{ij}]$  and call  $\mathbf{G}$  the *social proximity matrix*. Some assumptions on  $\mathbf{G}$  are introduced.

**Assumption 1.** *The social proximity matrix  $\mathbf{G} = [\psi_{ij}]$  satisfies the following property:*

- (a)  $\psi_{ij} \in (0, 1]$  for all  $i, j \in \mathcal{N}$  with  $\psi_{ii} = 1$ , and
- (b)  $\mathbf{z}^\top \mathbf{G} \mathbf{z} = \sum_{ij} \psi_{ij} z_i z_j > 0$  for any  $\mathbf{z} = (z_i)_{i \in \mathcal{N}}$  such that  $\sum_{i \in \mathcal{N}} z_i = 0$ .

Assumption 1 (a), in particular the positivity of every  $\psi_{ij}$ , simplifies the proof of existence of spatial equilibrium. It is not restrictive, since  $\psi_{ij}$  can be arbitrarily close to zero. Assumption 1 (b) is an assumption for interpretation and is less relevant in the theoretical analysis of the model. If the matrix  $\mathbf{G}$  satisfies Assumption 1 (b), then  $\mathbf{a}(\mathbf{x}) = (a_i(\mathbf{x}))_{i \in \mathcal{N}} = \mathbf{G}\mathbf{x}$  exhibits positive effects of agglomeration (see, e.g., Osawa and Akamatsu, 2019). For example, consider  $\mathbf{z} = \epsilon(\mathbf{e}_i - \mathbf{e}_j)$ , with  $\epsilon > 0$  and  $\mathbf{e}_i$  being  $i$ th standard basis. That is,  $\mathbf{z}$  represents infinitesimal relocation of workers from  $j$  to  $i$ . Under Assumption 1 (b), the gain in  $a_i$  induced by such a relocation vector  $\mathbf{z}$  is strictly greater than the gain in  $a_j$ , that is, we have  $a_i(\mathbf{x} + \mathbf{z}) - a_i(\mathbf{x}) > a_j(\mathbf{x} + \mathbf{z}) - a_j(\mathbf{x})$ . That is, relocation of workers induce *self-reinforcing* effects in terms of regional productivity.

Inter-regional transportation of differentiated goods is costly. We assume iceberg transportation costs, i.e.,  $\tau_{ij} \geq 1$  units should be shipped from  $i$  for a unit to arrive at  $j$ , with  $\tau_{ii} = 1$ . Under perfect competition, the price of the good produced in  $i$  and consumed in  $j$  is given by

$$p_{ij} = \frac{w_i}{a_i} \tau_{ij}. \quad (3.3)$$

A higher freeness of social interactions increases productivity and firms with higher worker productivity face lower marginal costs and thus charge a smaller optimal price  $p_{ij}$ . Under the CES assumption, the *value* shipped from location  $i$  to  $j$  is given by

$$Q_{ij} = \frac{p_{ij}^{1-\sigma}}{P_j^{1-\sigma}} w_j x_j, \quad (3.4)$$

where  $P_j$  is the CES price index:

$$P_j = \left( \sum_{i \in \mathcal{N}} p_{ij}^{1-\sigma} \right)^{\frac{1}{1-\sigma}} = \left( \sum_{i \in \mathcal{N}} a_i^{\sigma-1} w_i^{1-\sigma} \phi_{ij} \right)^{\frac{1}{1-\sigma}}, \quad (3.5)$$

with  $\phi_{ij} \equiv \tau_{ij}^{1-\sigma} \in (0, 1]$ . Below, we denote  $\mathbf{D} = [\phi_{ij}]$  and call  $\mathbf{D}$  the *geographical proximity matrix*. A key assumption here is that all entries of  $\mathbf{D}$  are strictly positive, i.e.,  $1 \leq \tau_{ij} < \infty$ , which would be natural:

**Assumption 2.**  $\phi_{ij} \in (0, 1]$  for all  $i, j \in \mathcal{N}$  with  $\phi_{ii} = 1$ .

We take Assumptions 1 and 2 to hold throughout the paper.

The regional price index is decreasing in  $a_i$ , implying that a higher freeness of social interactions decreases the cost of living in region  $i$ . As a result, global demand is increasing in the freeness of communications. Markets clear if the regional income is equal to the value of goods sold in all regions, that is, for all  $i \in \mathcal{N}$ :

$$w_i x_i = \sum_{k \in \mathcal{N}} Q_{ik} = \sum_{k \in \mathcal{N}} \frac{a_i^{\sigma-1} w_i^{1-\sigma} \phi_{ik}}{\sum_{l \in \mathcal{N}} a_l^{\sigma-1} w_l^{1-\sigma} \phi_{lk}} w_k x_k. \quad (3.6)$$

To normalize  $w$ , we assume that the total income of the economy is unity:

$$\sum_{i \in \mathcal{N}} w_i x_i = 1. \quad (3.7)$$

Suppose  $x$  is positive, that is,  $x_i > 0$  for all  $i \in \mathcal{N}$ . Then, there is unique wage vector  $w$  that solves market equilibrium conditions (3.6) and (3.7), which leads to the following Lemma.

**Lemma 1.** *There exists unique positive solution  $w$  to (3.6) and (3.7) at any positive spatial distribution  $x$ . For any  $i \in \mathcal{N}$ ,  $w_i \rightarrow \infty$  as  $x_i \rightarrow 0$ .*

See Appendix A for the proof. Below, all the proofs for the lemmas or propositions, and the associated technical derivations, are found in Appendix A.

In other words, (3.6) and (3.7) defines  $w$  as an implicit function of  $x$ . Also, the wage of worker in a region diverges as the mass of workers goes to zero.

With market wage  $w(x)$ , per capita indirect utility in region  $i$  is given by

$$v_i(x) = \frac{w_i(x)}{P_i(x)}, \quad (3.8)$$

where we emphasize that price index  $P_i$  is also a function of  $x$  through  $a(x)$  and  $w(x)$ . We use  $v(x) = (v_i(x))_{i \in \mathcal{N}}$  to denote the indirect utility, or the payoff, of workers as the function of the spatial distribution  $x$ . Wage  $w$  is differentiable in  $x$  due to the implicit function theorem; thus,  $v$  is differentiable whenever  $x_i > 0$  for all  $i \in \mathcal{N}$ .

The exogenous parameters of the model are elasticity of substitution  $\sigma > 1$ , geographical proximity matrix  $\mathbf{D}$ , and social proximity matrix  $\mathbf{G}$ . Given parameter values, a *spatial equilibrium* of the model is a spatial distribution  $x$  of workers, and its associated market wage  $w$  which satisfies (3.6), that equalizes utility of mobile workers across all regions. In other words, a spatial distribution  $x$  is a spatial equilibrium if no mobile worker in region  $i$  has an incentive to move to another region  $j \neq i$ . The next result establishes the existence of a spatial equilibrium.

**Proposition 1.** *There exists a spatial equilibrium for any  $\sigma > 1$ . All spatial equilibria are positive; all regions are populated at any spatial equilibrium.*

The model can thus exhibit the so-called “partial agglomeration.” Because there is positive demand for all varieties at any finite level of transportation cost under the Armington assumption and labor is the only input, the market wage of an individual worker diverges when the mass of workers in the same region goes to zero. Thus, the worker’s utility in such a region goes to infinity. Therefore, no spatial equilibrium can incorporate depopulated regions. We will illustrate this in Section 4 by numerical examples.

Since multiple equilibria may arise due to the centripetal force embedded by  $a(\cdot)$ , we consider equilibrium refinement based on some myopic dynamics  $\dot{x} = f(x)$ . We focus on dynamics of the form  $\dot{x} = f(x) = f(x, v(x))$ , i.e., the dynamics that maps spatial distribution  $x$  and payoff level  $v(x)$  to a motion vector. We assume that  $f$  and  $\tilde{f}$  are differentiable for all positive  $x$  and satisfy (i)  $f(x) = \mathbf{0}$  if and only if  $x$  is a spatial equilibrium of our model and (ii) if  $f(x) \neq \mathbf{0}$ , then  $v(x)^\top f(x) > 0$ , and (iii)  $\mathbf{P}f(x, v(x)) = f(\mathbf{P}x, \mathbf{P}v(x))$  for all permutation matrices  $\mathbf{P}$ . Conditions (i) and (ii) are, respectively, called *Nash stationality* and *positive correlation* (Sandholm, 2010), which are the most parsimonious assumptions we can impose on a dynamic  $f$  to be “consistent” with the underlying model (payoff function)  $v$ . Condition (iii) ensures that  $f$  is not biased, i.e., it does not ex-ante prefer some regions to the others. In other words, we suppose that all location incentives

for workers are captured by the payoff function. We suppose  $f$  is  $C^1$ , only because we employ linear stability as the definition of stability. We call dynamics that satisfy conditions (i), (ii), and (iii) *admissible dynamics*.

Admissible dynamics include, for instance, the *Brown–von Neumann–Nash dynamic* (Brown and von Neumann, 1950; Nash, 1951), the *Smith dynamic* (Smith, 1984), the *Euclidian projection dynamic* (Dupuis and Nagurney, 1993), and the *replicator dynamic* (Taylor and Jonker, 1978). See Sandholm (2010) for more examples. The replicator dynamic, which is a standard choice in the economic geography literature, is defined as

$$\dot{x}_i = f_i(\mathbf{x}, \mathbf{v}(\mathbf{x})) \equiv \left( v_i(\mathbf{x}) - \sum_{k \in \mathcal{N}} x_k v_k(\mathbf{x}) \right) x_i. \quad (3.9)$$

The dynamic can violate condition (i) in general payoff functions  $\mathbf{v}(\mathbf{x})$ . However, it satisfies condition (i) in the interior of  $\mathcal{X}$  and is hence applicable to our model, since spatial equilibria are always interior. The stability claims in the rest of the paper hold true for any admissible dynamics.

We show general properties at the extremal values of transportation costs. Obviously, the uniform distribution of workers across regions is an equilibrium if trade and social interactions are completely frictionless. We formalize as follows.

**Proposition 2.** *Consider the “death-of-distance” limit where trade and social interactions between different regions are completely costless, i.e., the limit when  $\phi_{ij} \rightarrow 1$  and  $\psi_{ij} \rightarrow 1$  for all  $i, j \in \mathcal{N}$ . Then, the uniform distribution  $\bar{\mathbf{x}} = (\bar{x}, \bar{x}, \dots, \bar{x})$  with  $\bar{x} \equiv \frac{1}{n}$  is the unique and stable spatial equilibrium.*

On the other hand, in the converse limit where trade and social interactions are too costly, the only stable equilibria are full agglomeration towards one of the regions.

**Proposition 3.** *Consider the “autarky” limit where trade and social interactions between different regions are prohibitively costly, i.e., the limit when  $\phi_{ij} \rightarrow 0$  and  $\psi_{ij} \rightarrow 0$  for all  $i \neq j$ . Stable equilibrium spatial patterns are full agglomeration in one of the regions, that is,  $x_i = 1$  for some  $i \in \mathcal{N}$  and  $x_j = 0$  for all  $j \neq i$ .*

Propositions 2 and 3 show that the economy exhibits a *dispersion process* from a mono-centric configuration when transportation costs decline. We will confirm this through examples in Sections 4 and 5. Proposition 3 demonstrates that there are possibility of multiple equilibria, as expected.

Below, we explore concrete examples which are designed to illustrate the essential implications of considering the social proximity structure. Section 4 considers the canonical starting point, the symmetric two regions. Section 5 considers four-region setups with various social proximity structure  $\mathbf{G}$  to investigate the role of the network structure.

## 4 Dispersion process in a two-region economy

As usual, we start with the simplest possible setup — the symmetric two regions — to elucidate basic workings of the model. We study the stability of the symmetric equilibrium, i.e., the uniform distribution. In particular, we show that the uniform distribution is stable when transportation of goods are freer, which is akin to the model by Helpman (1998). In our model, there is another proximity measure: the freeness of social interactions between the two regions.

When the regions are symmetric, it is natural to assume that

$$\mathbf{D} = \begin{bmatrix} 1 & \phi \\ \phi & 1 \end{bmatrix} \quad \text{and} \quad \mathbf{G} = \begin{bmatrix} 1 & \psi \\ \psi & 1 \end{bmatrix}, \quad (4.1)$$

where  $\phi \in (0, 1)$  and  $\psi \in (0, 1)$ . We call  $\phi$  the *freeness of trade* and  $\psi$  the *freeness of communication*. It is easy to see that the uniform distribution  $\bar{x} \equiv (\bar{x}, \bar{x})$  with  $\bar{x} = \frac{1}{2}$  is a spatial equilibrium for all  $(\sigma, \phi, \psi)$ . We have  $w_1 = w_2 = 1$  and  $v_1(\bar{x}) = v_2(\bar{x}) = \bar{v} \equiv (1 + \psi)(1 + \phi)^{\frac{1}{\sigma-1}} \bar{x} > 0$  at  $\bar{x}$ .

The symmetric distribution  $\bar{x}$  is stable (unstable) if the utility gain for an agent relocating from one region to the other is negative (positive). In the two-region economy, the gain for a hypothetical migrant can be evaluated by the following elasticity:

$$\omega = \frac{\bar{x}}{\bar{v}} \frac{\partial(v_1 - v_2)}{\partial x_1}(\bar{x}) = \frac{\bar{x}}{\bar{v}} \left( \frac{\partial v_1}{\partial x_1}(\bar{x}) - \frac{\partial v_2}{\partial x_1}(\bar{x}) \right). \quad (4.2)$$

The gain  $\omega$  is a positive scalar multiple  $\left(\frac{\bar{x}}{\bar{v}}\right)$  of an eigenvalue of the Jacobian matrix of  $v(x)$  at  $\bar{x}$ . Multiplying  $\frac{\bar{x}}{\bar{v}} > 0$  simplifies the formulae in what follows.

If  $\omega < 0$ , then  $\bar{x}$  is stable because there is no incentive for agents to migrate; if  $\omega > 0$ , a marginal increase in the mass of workers in a region induces a *relative decrease* of the per capita utility therein. Similarly,  $\bar{x}$  is unstable if  $\omega > 0$ ; when a small fraction of workers relocate from region 2 to 1, then it induces a *relative increase* of the payoff in region 1, encouraging further migration from region 2. Thus, if we start from a state where  $\bar{x}$  is stable ( $\omega < 0$ ), endogenous agglomeration emerges when the gain turns to positive ( $\omega > 0$ ).

We can evaluate  $\omega$  as follows:

$$\omega = \Omega(\chi, \lambda) \equiv \frac{-1 + \chi + ((\sigma - 1) + \sigma\chi) \lambda}{\sigma + (\sigma - 1)\chi}, \quad (4.3)$$

where  $\chi \in (0, 1)$  and  $\lambda \in (0, 1)$  are respectively defined by

$$\chi \equiv \frac{1 - \phi}{1 + \phi} \quad \text{and} \quad \lambda \equiv \frac{1 - \psi}{1 + \psi}. \quad (4.4)$$

The variables  $\chi$  and  $\lambda$  are, respectively, the eigenvalues of row-normalized proximity matrices  $\frac{1}{1+\phi}\mathbf{D}$  and  $\frac{1}{1+\psi}\mathbf{G}$ , with the associated eigenvector being  $z = (1, -1)$ .

As it turns out,  $\Omega$  plays a major role in our analysis of the model.<sup>1</sup> The variables  $\chi$  and  $\lambda$  can be understood as, respectively, indices of trade costs and interaction costs. For instance,  $\chi$  is decreasing in  $\phi$ , that is,  $\chi$  is large (small) when trade barriers are high (low). Note that the denominator of  $\omega$  is positive for all admissible values of  $\sigma$  and  $\phi$ .

The numerator of  $\omega$  reveals the net agglomeration and dispersion forces in the model. The first term is negative and thus represents the dispersion force due to costly trade. In particular, if  $\mathbf{a}$  is a constant vector that does not depend on the spatial distribution of workers, then  $\lambda = 0$  and thus  $\omega < 0$ . That is,  $\bar{x}$  is always stable if  $\mathbf{a}$  is constant. This is simply because, without any agglomerative forces, costly trade of goods discourages uneven concentration of workers. Also,

<sup>1</sup>In the context of economic geography models with no social proximity structure, Akamatsu et al. (2019) calls  $\Omega$  that satisfies  $\omega \equiv \Omega(\chi)$  the *gain function* of a model.

we see that the dispersion force *strengthens* when  $\phi$  increases, since  $\chi$  is decreasing in  $\phi$ . Because every region specializes on a single variety, workers' love for variety due to the CES preferences induces a stronger centrifugal force when trade is freer. The second term is positive and represents the agglomerative force due to the productivity spillover (3.2). Because  $\lambda \in (0, 1)$  is monotonically decreasing in  $\psi$ , this force is at its strongest when  $\psi$  is small, which is intuitive.

To obtain more insights, we may break down  $\omega$  as follows:

$$\omega = \epsilon_a \alpha_x + \epsilon_w \beta_x, \quad (4.5)$$

where  $\epsilon_a$  and  $\epsilon_w$  are the following elasticities of payoff difference  $v_1 - v_2$  with respect to, respectively,  $a_1$  and  $w_1$  at  $x = \bar{x}$ :

$$\epsilon_a \equiv \frac{\bar{a}}{\bar{v}} \left( \frac{\partial v_1}{\partial a_1}(\bar{x}) - \frac{\partial v_2}{\partial a_1}(\bar{x}) \right) \quad \text{and} \quad \epsilon_w \equiv \frac{\bar{w}}{\bar{v}} \left( \frac{\partial v_1}{\partial w_1}(\bar{x}) - \frac{\partial v_2}{\partial w_1}(\bar{x}) \right), \quad (4.6)$$

with  $\bar{a} \equiv a_1(\bar{x}) = \bar{a}(1 + \psi)$  and  $\bar{w} = 1$  being the uniform levels of regional productivity and wage. Also,  $\alpha_x$  and  $\beta_x$  are, respectively, the following elasticities of  $a_1$  and  $w_1$  with respect to migration of workers from one region to the other:

$$\alpha_x \equiv \frac{\bar{x}}{\bar{a}} \left( \frac{\partial a_1}{\partial x_1}(\bar{x}) - \frac{\partial a_1}{\partial x_2}(\bar{x}) \right) \quad \text{and} \quad \beta_x \equiv \frac{\bar{x}}{\bar{w}} \left( \frac{\partial w_1}{\partial x_1}(\bar{x}) - \frac{\partial w_1}{\partial x_2}(\bar{x}) \right). \quad (4.7)$$

Note that regions are interchangeable, so we can swap the indices in the above expressions.

At the uniform distribution  $\bar{x}$ , we can evaluate as follows:

$$\epsilon_a = \chi, \quad \epsilon_w = 1 - \chi, \quad \alpha_x = \lambda, \quad \text{and} \quad \beta_x = \frac{(\sigma - 1)(1 + \chi)\lambda - 1}{\sigma + (\sigma - 1)\chi}. \quad (4.8)$$

All the first three elasticities are positive and thus migration of workers tends to cause positive circular causality and thus destabilize  $\bar{x}$ . When trade is more costly ( $\phi$  is small and thus  $\chi$  is large), then the payoff difference is more sensitive to the variation in productivity ( $\epsilon_a$  is large), whereas it is less sensitive to wage ( $\epsilon_w$  is small). Also, a region's productivity is sensitive to migration when social interactions are costly because  $\alpha_x = \lambda$  is large when  $\psi$  is small.

Only the last elasticity,  $\beta_x$ , can be negative and produce a stabilizing effect. It is negative when  $(\sigma - 1)(1 + \chi)\lambda < 1$ , that is, when  $\psi$  and  $\phi$  are sufficiently large (and/or  $\sigma$  is sufficiently small). In fact,  $\beta_x$  can be further decomposed as follows:

$$\beta_x = \zeta_a \alpha_x + \zeta_x = \lambda \zeta_a + \zeta_x, \quad (4.9)$$

where  $\zeta_a$  and  $\zeta_x$  are the elasticities of nominal wage difference  $w_1 - w_2$  respect to, respectively, the productivity in region 1 and the mass of worker in region 1 and are given as follows:

$$\zeta_a \equiv \frac{\bar{a}}{\bar{w}} \left( \frac{\partial w_1}{\partial a_1}(\bar{x}) - \frac{\partial w_2}{\partial a_1}(\bar{x}) \right) = \frac{(\sigma - 1)(1 + \chi)}{\sigma + (\sigma - 1)\chi} > 0 \quad (4.10)$$

$$\zeta_x \equiv \frac{\bar{x}}{\bar{w}} \left( \frac{\partial w_1}{\partial x_1}(\bar{x}) - \frac{\partial w_2}{\partial x_1}(\bar{x}) \right) = -\frac{1}{\sigma + (\sigma - 1)\chi} < 0. \quad (4.11)$$

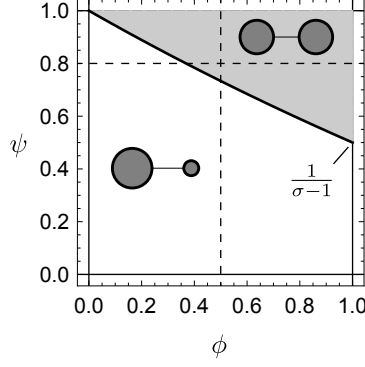


**Figure 1:** Stability of  $\bar{x}$  in the two-region economy ( $\sigma = 4.0$ ).

*Notes:* The uniform distribution  $\bar{x}$  is stable for the shaded (gray) region of  $(\phi, \psi)$  and the black solid curve indicates the critical pair of  $(\phi, \psi)$  where  $\bar{x}$  becomes unstable. The horizontal and vertical dashed lines correspond to the parametric paths for the bifurcation diagrams Figure 2a and Figure 2b, respectively. The schematic on each (gray or white) parametric region indicates the representative spatial pattern in the parametric region.

We see that  $\zeta_a > 0$ . A population increase in region 1 induces relative productivity increase  $\alpha_x = \lambda > 0$ , which in turn gives rise to an increase in nominal wage in the region since  $\zeta_a \alpha_x > 0$ . On the other hand,  $\zeta_w < 0$ . If the mass of worker in a region increases, then it brings about a negative effect on nominal wage since the total revenue in a region is given by  $w_i x_i$ . The single value  $\omega$  thus captures the net effect through the combination of all the effects discussed above.

With the formula of  $\omega$ , we have the following characterization of the stability of  $\bar{x}$ .

**Proposition 4.** *Suppose  $n = 2$ . Assume **D** and **G** in (4.1). Then, the uniform distribution  $\bar{x} = (\bar{x}, \bar{x})$  is linearly stable if and only if  $\omega = \Omega(\chi, \lambda) < 0$ .*

Figure 1 shows Proposition 4 on the  $(\phi, \psi)$ -space. For illustration, we let  $\sigma = 4.0$ ; the results remain invariant under a reasonable range of values for sigma.<sup>2</sup> The stability condition  $\omega < 0$  is satisfied when both  $\phi$  and  $\psi$  are relatively high. The black solid curve shows the critical pairs of  $(\phi, \psi)$  below which  $\bar{x}$  becomes unstable, i.e., the solutions for  $\omega(\phi, \psi) = \Omega(\chi(\phi), \lambda(\psi)) = 0$ . The uniform distribution  $\bar{x}$  is stable in the shaded areas of  $(\phi, \psi)$ , and unstable otherwise. For any  $\phi \in (0, 1)$ ,  $\bar{x}$  is stable when the freeness of social interactions  $\psi$  is sufficiently high. When  $\psi$  is small and inter-region communication is lower, agents tend to agglomerate due to positive externalities.

Let  $\phi^*$  be the critical value of  $\phi$  at which  $\bar{x}$  becomes unstable. In terms of  $\sigma$  and  $\psi$ , the critical value is given as follows:

$$\phi^* = (2\sigma - 1) \frac{\lambda}{2 + \lambda} = (2\sigma - 1) \frac{1 - \psi}{3 + \psi} > 0. \quad (4.12)$$

If  $\phi^* \in (0, 1)$ , then the uniform distribution is stable for all  $\phi \in (\phi^*, 1)$ . If otherwise  $\phi^* \geq 1$ , then  $\bar{x}$  is unstable for all  $\phi \in (0, 1)$ , so that the economy always exhibits asymmetry (e.g.,  $x_1 > x_2$ ). For this reason, the requirement that  $\phi^* \in (0, 1)$  may be called “no-black-hole” condition following Fujita et al. (1999). We have  $\phi^* \in (0, 1)$  either when  $\sigma \in (1, 2)$  (which is unrealistic) or when  $\sigma \geq 2$  and  $\psi > \frac{\sigma-2}{\sigma}$ . If instead  $\psi \leq \frac{\sigma-2}{\sigma}$ , then  $\bar{x}$  is unstable for any  $\phi$ . It is natural that when the

<sup>2</sup>See Appendix B.

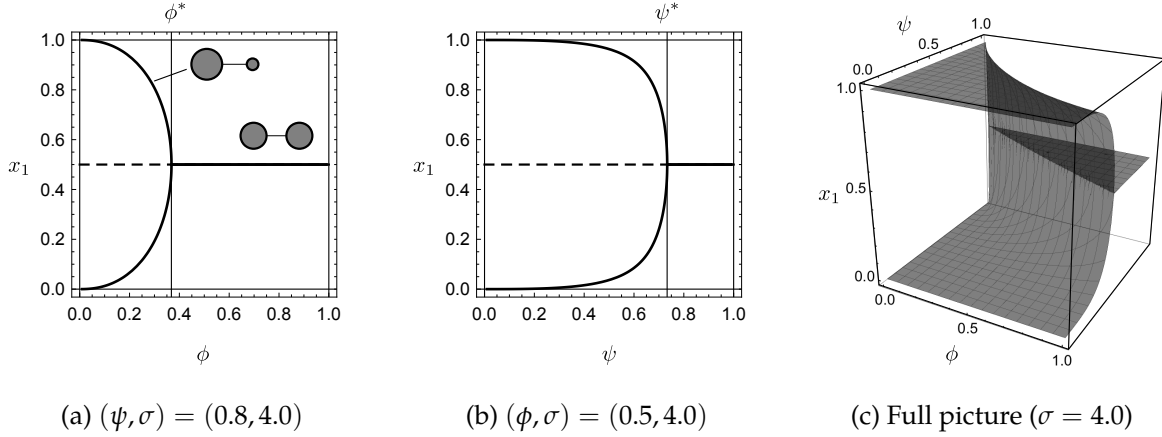


**Figure 2:** Bifurcation diagrams for the symmetric two-region economy.

*Notes:* In Figures 2a and 2b, the black solid curves indicate stable spatial equilibria, whereas dashed curves indicate unstable ones. The schematics by the black solid curve show the spatial configurations, where the size of each gray disk indicates the size of a region. In Figure 2c, the transparent gray surface indicates the stable equilibria in terms of  $x_1$ . Figures 2a and 2b are the cross sections of the surface at, respectively,  $\psi = 0.8$  and  $\phi = 0.5$ . We can consider various cross sections of the surface, or curves over the  $(\phi, \psi)$ -space, to investigate the effects of simultaneous changes in  $(\phi, \psi)$ .

elasticity of substitution  $\sigma$  is relatively large and the freeness of interaction  $\psi$  is relatively small, then migration towards one of the regions is profitable.

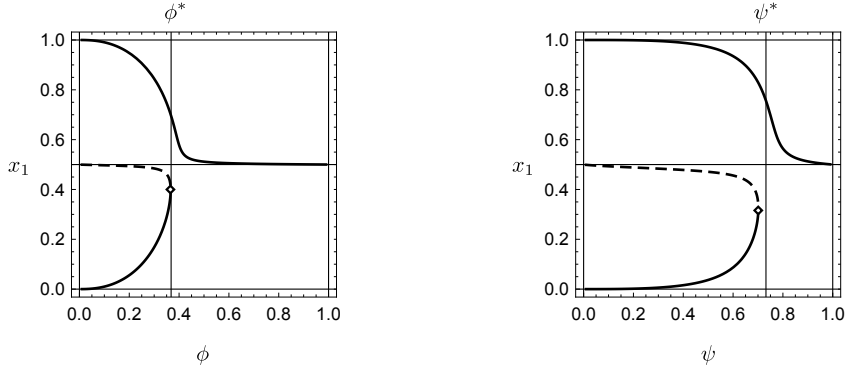
When the threshold value  $\phi^*$  (or that in terms of  $\psi$ ) is attained, the uniform distribution becomes unstable and endogenous agglomeration emerges. Figure 2 shows the bifurcation diagram of stable spatial equilibria in terms of  $x_1$  when  $\phi$  and/or  $\psi$  varies. Figures 2a and 2b show, respectively, the bifurcation diagrams for the horizontal and vertical dashed lines in Figure 1. Figure 2c shows the bifurcation diagram of stable equilibrium values of  $x_1$  over the full  $(\phi, \psi)$ -space. The uniform distribution is stable for high values of  $\phi$  or  $\psi$ , and the stable paths are continuous in transportation cost parameter axes. Thus, the model highlights the process of the resolution of an established agglomeration when  $\phi$  and/or  $\psi$  monotonically increases. This is akin to Helpman (1998)'s model, with an additional dimension of social proximity  $\psi$ . There are no catastrophic jumps nor hysteresis when  $\bar{x}$  becomes unstable, which is also similar to Helpman (1998) and others. We can formally show that the bifurcation from  $\bar{x}$  is a supercritical pitchfork, which essentially means that the dispersion process is “reversible.”

**Proposition 5.** *The bifurcation from  $\bar{x}$  in the course of decreasing  $\phi$ , or decreasing  $\psi$ , is of the supercritical pitchfork form. The dispersion process of economic activities is smooth and gradual as the economy becomes more symmetric.*

Asymmetries in the proximity matrices ( $\mathbf{D}$  and  $\mathbf{G}$ ) induce straightforward comparative advantages. Figure 3 shows examples in which the two regions are asymmetric. In Figures 3a and 3b, we respectively assume  $\mathbf{D}$  and  $\mathbf{G}$  of the form

$$\mathbf{D} = \begin{bmatrix} 1 & \phi^{1.1} \\ \phi & 1 \end{bmatrix} \quad \text{and} \quad \mathbf{G} = \begin{bmatrix} 1 & \psi \\ \psi^{1.1} & 1 \end{bmatrix}. \quad (4.13)$$

For both the cases, region 1 has comparative advantage (in terms of cost of living or productivity).



(a)  $(\psi, \sigma) = (0.8, 4.0)$ ,  $\phi_{12} = \phi^{1.1} < \phi$       (b)  $(\phi, \sigma) = (0.5, 4.0)$ ,  $\psi_{21} = \psi^{1.1} < \psi$

**Figure 3:** Bifurcation diagrams for the asymmetric two-region economy.

*Notes:* Black solid curves indicate stable spatial equilibria, whereas dashed curves unstable ones. The diamond ( $\diamond$ ) in each figure indicates the limit point from which a pair of unstable and stable equilibria emerge.  $\phi^*$  and  $\psi^*$  indicate the critical values for the symmetric setups shown in Figure 2.

The bifurcation diagrams exhibit the standard unfolding behavior for the supercritical pitchfork bifurcation, for which transition on the main path (the path with  $x_1 > x_2$ ) is smooth without any catastrophic behaviors. The economy is always asymmetric and the uniform distribution emerges only in the limits  $\phi \rightarrow 1$  or  $\psi \rightarrow 1$ .

## 5 How the network structure of social proximity matters

We now turn our attention to a multi-region geography with more than two regions to identify two quintessential roles of the social proximity structure  $\mathbf{G}$ : (i) one on the timing of dispersion; and (ii) the other on the overall spatial distribution of workers.

This section considers a symmetric four-region geography in which  $n = 4$  regions are equidistantly placed over a circular transportation network (see Figure 4), as in Matsuyama (2017), Example 2. This is a simplified version of the 12-location race-track economy of Krugman (1993). It is the minimal symmetric geographical environment in which different regions have different neighbors (three is not enough). By postulating that the transportation of goods is only possible over the circular network, we can assume that the geographical proximity matrix is given by

$$\mathbf{D} = \begin{bmatrix} 1 & \phi & \phi^2 & \phi \\ & 1 & \phi & \phi^2 \\ & & 1 & \phi \\ \text{Sym.} & & & 1 \end{bmatrix}, \quad (5.1)$$

where  $\phi \in (0, 1)$  is the freeness of trade between two consecutive regions over the economy.

Four is also the minimal number that allow nontrivial structures of social interactions between locations. Taking  $\mathbf{D}$  in (5.1) as given, we consider three stylized settings for  $\mathbf{G}$ , shown in Figure 5, to elucidate the basic roles of the social proximity structure. Figure 5a shows the baseline case where the movement of people is governed by a similar transportation technology as goods trade (e.g.,

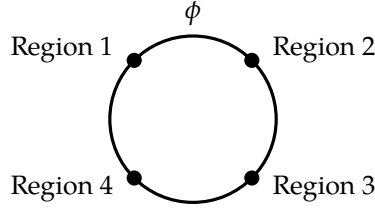


**Figure 4:** Four-region symmetric geography.

*Notes:* The black circle represents the transportation network, whereas the black markers represent the regions. All regions have the same level of geographical proximity to the other regions.

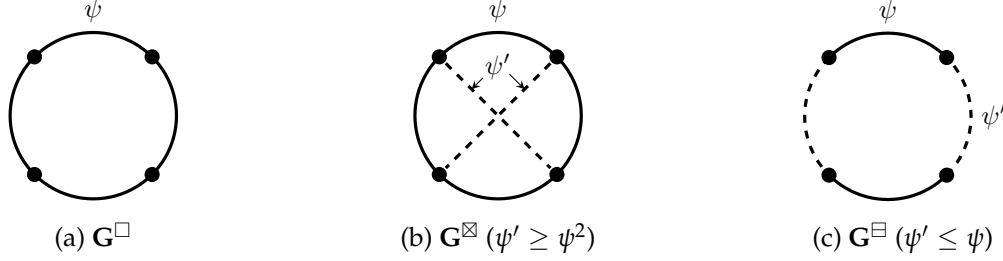


**Figure 5:** Various social proximity structures in the symmetric four-region geography.

*Notes:* (a) The baseline case where the movement of people is governed by a similar transportation technology as goods trade (e.g., highways, low-speed railways). (b) A case where the pairs of regions at the antipodal locations are socially close (due to some transportation modes specialized to passenger trips, e.g., high-speed railways, regional airlines). (c) A case where the social proximity matrix have a hierarchical structure (due to, e.g., intra-country developments of passenger transports before an economic integration).

highways, low-speed railways). Figure 5b represents a case where there are some transportation modes specialized to passenger trips such as regional airlines, which tend to shorten travel time across distant locations. Figure 5c is a case where the passenger transportation modes has a block structure due to, e.g., intra-country developments before a major economic integration.

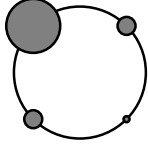
The social proximity matrices for the three cases are, respectively, given as follows:

$$\mathbf{G}^{\square} = \begin{bmatrix} 1 & \psi & \psi^2 & \psi \\ & 1 & \psi & \psi^2 \\ & & 1 & \psi \\ \text{Sym.} & & & 1 \end{bmatrix}, \quad \mathbf{G}^{\boxtimes} = \begin{bmatrix} 1 & \psi & \psi' & \psi \\ & 1 & \psi & \psi' \\ & & 1 & \psi \\ \text{Sym.} & & & 1 \end{bmatrix}, \quad \text{and } \mathbf{G}^{\square} = \begin{bmatrix} 1 & \psi & \psi'\psi & \psi' \\ & 1 & \psi' & \psi'\psi \\ & & 1 & \psi \\ \text{Sym.} & & & 1 \end{bmatrix} \quad (5.2)$$

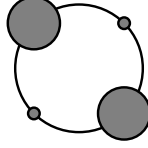
where  $\psi \in (0, 1)$  and  $\psi' \in (0, 1)$ . For  $\mathbf{G}^{\boxtimes}$ , we assume  $\psi' > 2\psi - 1$  to satisfy Assumption 1 (b). In fact,  $\mathbf{G}^{\square}$  is a special case of  $\mathbf{G}^{\boxtimes}$  where  $\psi' = \psi^2$ . For  $\mathbf{G}^{\square}$ , we assume  $\psi' \leq \psi$  without loss of generality.

All regions have the same level of geographical proximity to the other regions under  $\mathbf{D}$  in (5.1). Also, for any  $\mathbf{G}^{\square}$ ,  $\mathbf{G}^{\boxtimes}$ , and  $\mathbf{G}^{\square}$ , the social proximity matrix does not induce any ex-ante comparative advantage of regions and preserves the symmetry of the four-region economy. Thus, uniform distribution  $\bar{x} = (\bar{x}, \bar{x}, \bar{x}, \bar{x})$  with  $\bar{x} \equiv \frac{1}{4}$  is a spatial equilibrium for any  $(\sigma, \phi, \psi, \psi')$ . In the following, we study the stability of  $\bar{x}$  and endogenous agglomeration from  $\bar{x}$ .

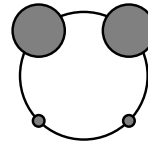
An important difference from the two-region case is that there are three qualitatively distinct migration patterns when  $\bar{x}$  becomes unstable. Figure 6 schematically shows the three possible



(a) Mono-centric pattern



(b) Duo-centric pattern



(c) North–South pattern

**Figure 6:** Schematics of the possible endogenous outcomes in the symmetric four-region economy.

*Notes:* The black circle indicates the transportation network. Each gray disk represents the population size of each region. We do not show rotationally symmetric patterns that are essentially equivalent to the three patterns shown above (e.g., the “East–West” pattern).

outcomes. These migration patterns are, in fact, the eigenvectors of the Jacobian matrix of the payoff function at  $\bar{x}$ . Figure 6a and Figure 6c correspond to the formation of a mono-centric spatial distribution where one region or two contiguous regions attract the majority of workers. The latter may be called the “North–South” pattern. Figure 6b corresponds to the emergence of duo-centric configuration where two geographically remote regions are vying with each other.

A more “realistic” setup is the star-shaped network, where one of the regions — maybe the host of the capital city — is the hub for the social interactions in the economy. For example, when region 1 is connected symmetrically to all the other regions but there is no direct interaction path between regions 2, 3, and 4, we have

$$\mathbf{G}^\star = \begin{bmatrix} 1 & \psi & \psi & \psi \\ & 1 & \psi^2 & \psi^2 \\ & & 1 & \psi^2 \\ \text{Sym.} & & & 1 \end{bmatrix}. \quad (5.3)$$

This assumption induces an exogenous advantage in region 1, thereby the results are straightforward (cf. the asymmetric cases in Section 4). That is, the spatial pattern becomes mono-centric, with region 1 as the central location. We instead focus on symmetric networks where no region has exogenous advantages in terms of proximity to the other regions.

## 5.1 The baseline case and endogenous agglomeration in many-region settings

This section considers the most straightforward assumption,  $\mathbf{G}^\square$  (Figure 5a), where the social proximity matrix has a similar structure to the geographical proximity matrix  $\mathbf{D}$ . This setup is related to geographically decaying spillovers considered in urban economics models.

In many-region settings to be considered in Section 5, the stability of  $\bar{x} = (\bar{x}, \bar{x}, \bar{x}, \bar{x})$  is governed by the *largest eigenvalue* of the payoff elasticity matrix  $\mathbf{V} = \frac{\bar{x}}{\bar{v}} \nabla v(\bar{x})$ . To see this, suppose that  $\bar{x}$  is perturbed to become  $x' = \bar{x} + z$  with small  $z = (z_i)_{i \in \mathcal{N}}$ , where  $z^\top \mathbf{1} = \sum_{i \in \mathcal{N}} z_i = 0$  because the total population is constant. In other words,  $z$  is a migration pattern. The average gain (in terms of relative payoff) induced by such a deviation is

$$\bar{\omega}(z) \equiv z^\top \mathbf{V} z \quad (5.4)$$

because we show, via linearization  $v(\mathbf{x}') \approx v(\bar{\mathbf{x}}) + \nabla v(\bar{\mathbf{x}})\mathbf{z}$ , that the elasticity of average payoff  $\sum_{i \in \mathcal{N}} v_i(\mathbf{x})x_i$  is computed as

$$\frac{\bar{x}}{\bar{v}} \left( \sum_{i \in \mathcal{N}} v_i(\mathbf{x}')x'_i - \sum_{i \in \mathcal{N}} v_i(\bar{\mathbf{x}})\bar{x}_i \right) \approx \mathbf{z}^\top \mathbf{V}\mathbf{z}. \quad (5.5)$$

If  $\bar{\omega}(\mathbf{z}) < 0$  for *any* perturbation  $\mathbf{z}$ , then any form of migration is strictly non-profitable for migrants and hence  $\bar{\mathbf{x}}$  is stable.

Appendix A.2 shows that the average gain  $\bar{\omega}$  is maximized by deviation of the form  $\mathbf{z} = \mathbf{z}^*$ , where  $\mathbf{z}^*$  is the eigenvector of  $\mathbf{V}$  associated with its largest eigenvalue,  $\omega^* \equiv \max_k \{\omega_k\}$ . That is, we have

$$\max_{\mathbf{z}} \bar{\omega} = \bar{\omega}(\mathbf{z}^*) = \omega^*, \quad (5.6)$$

where  $\{\omega_k\}$  are the eigenvalues of  $\mathbf{V}$ . If  $\omega^* < 0$ , then  $\bar{\omega} < 0$  for any  $\mathbf{z}$ . When  $\omega^*$  switches from negative to positive, then migration towards  $\mathbf{z}^*$ -direction becomes profitable for workers and the spatial pattern of the form  $\mathbf{x}' = \bar{\mathbf{x}} + \epsilon \mathbf{z}^*$  ( $\epsilon > 0$ ) emerges.

When  $\mathbf{G} = \mathbf{G}^\square$ , we have

$$\mathbf{z}^* = (1, 0, -1, 0), \quad (5.7)$$

which is an eigenvector of  $\mathbf{V}$ . We have  $\omega^* \mathbf{z}^* = \mathbf{V}\mathbf{z}^* = \mathbf{V}^\top \mathbf{z}^*$  and thus

$$\omega^* = \frac{\bar{x}}{\bar{v}} \left( \frac{\partial v_1}{\partial x_1}(\bar{\mathbf{x}}) - \frac{\partial v_3}{\partial x_1}(\bar{\mathbf{x}}) \right). \quad (5.8)$$

Analogous to (4.2), (5.8) indicates that the migration from region 3 to 1 is profitable for workers. Thus, when  $\omega^*$  turns from negative, the spatial pattern becomes a mono-centric pattern of the form  $\mathbf{x}' = \bar{\mathbf{x}} + \epsilon \mathbf{z}^* = (\bar{x} + \epsilon, \bar{x}, \bar{x} - \epsilon, \bar{x})$ , as in Figure 6a.

The above discussion generalizes the two-region investigation where we employ gain  $\omega$ . When  $n = 2$ ,  $\omega$  is the only relevant eigenvalue of  $\mathbf{V}$  and  $\mathbf{z}^* = (1, -1)$ . Endogenous agglomeration is essentially  $\mathbf{x} = \bar{\mathbf{x}} + \epsilon \mathbf{z}^* = (\bar{x} + \epsilon, \bar{x} - \epsilon)$ .

The next proposition characterizes the stability of  $\bar{\mathbf{x}}$  and endogenous agglomeration from it.

**Proposition 6.** *Suppose  $n = 4$ . Assume  $\mathbf{D}$  in (5.1) and  $\mathbf{G} = \mathbf{G}^\square$ . Then,  $\omega^* = \Omega(\chi, \lambda)$  and  $\mathbf{z}^* = (1, 0, -1, 0)$ . The uniform distribution  $\bar{\mathbf{x}}$  is linearly stable if and only if  $\omega^* < 0$ . When  $\bar{\mathbf{x}}$  becomes unstable, then a mono-centric pattern of the form  $\bar{\mathbf{x}} + \epsilon \mathbf{z}^*$  ( $\epsilon > 0$ ) emerges.*

Figure 6a shows the endogenous spatial pattern under this setting. In Proposition 6,  $\chi$  and  $\lambda$  are the same as Proposition 4, that is,  $\chi = \frac{1-\phi}{1+\phi}$  and  $\lambda = \frac{1-\psi}{1+\psi}$ . These are, in fact, the eigenvalues of the row-normalized proximity matrices

$$\bar{\mathbf{D}} \equiv \frac{1}{1+2\phi+\phi^2} \mathbf{D} \quad \text{and} \quad \bar{\mathbf{G}}^\square \equiv \frac{1}{1+2\psi+\psi^2} \mathbf{G}^\square, \quad (5.9)$$

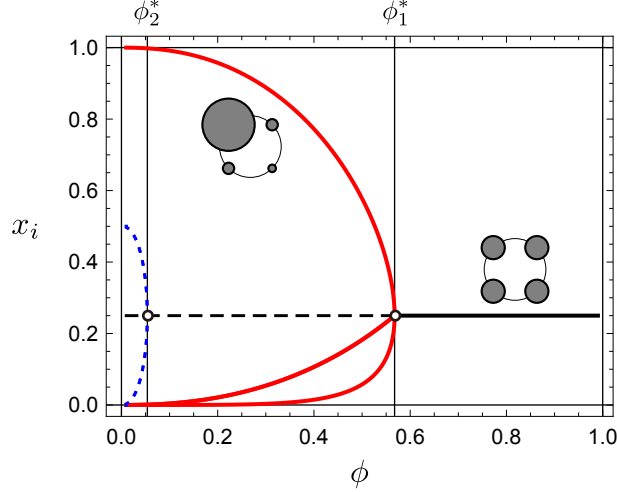


**Figure 7:** Bifurcation diagram for the four-region circular economy with social proximity matrix  $\mathbf{G}^\square$ .

*Notes:*  $\psi = 0.7$  and  $\sigma = 4$ . The solid curves indicate stable equilibria, whereas the dashed curves indicate unstable ones. The red curve corresponds to a mono-centric pattern (stable), whereas the blue curve is a duo-centric pattern (unstable). The schematics by the solid curves show representative snapshots of associated stable spatial patterns.

since we have

$$\bar{\mathbf{D}}\mathbf{z}^* = \frac{1 - \phi^2}{1 + 2\phi + \phi^2}\mathbf{z}^* = \frac{1 - \phi}{1 + \phi}\mathbf{z}^* \quad \text{and} \quad \bar{\mathbf{G}}^\square\mathbf{z}^* = \frac{1 - \psi^2}{1 + 2\psi + \psi^2}\mathbf{z}^* = \frac{1 - \psi}{1 + \psi}\mathbf{z}^*, \quad (5.10)$$

where  $\chi$  and  $\lambda$  can be seen as, again, the measures of transportation and interaction costs in the economy. As seen,  $\omega^*$  is computed via  $(\chi, \lambda)$  and  $\Omega$ , similar to the  $n = 2$  case.

Figure 7 shows the bifurcation diagram for  $\mathbf{G} = \mathbf{G}^\square$  in the  $\phi$ -axis. The levels of  $\phi$  at which  $\omega_1 = 0$  and  $\omega_2 = 0$  are indicated by, respectively,  $\phi_1^*$  and  $\phi_2^*$ . We have  $\omega^* = \max\{\omega_1, \omega_2\} = \omega_1$  for any  $(\phi, \psi, \sigma)$ . As discussed in the two-region case, the dispersion force due to costly trade, the first term in  $\Omega(\chi, \lambda)$ , is triggered when  $\phi$  is high. When  $\phi$  is in its lower extreme ( $\phi \rightarrow 0$ ), workers can concentrate in a single region because the dispersion force is less important. The spatial pattern is close to the complete agglomeration, e.g.,  $\mathbf{x} \approx (1, 0, 0, 0)$ , which is consistent with Proposition 3. As  $\phi$  increases, the relative rise of the dispersion force induces a crowding-out from the populated region. The spatial pattern become, e.g.,  $\mathbf{x} = (x, x', x'', x')$  with  $x > x' > x''$ , which is a mono-centric pattern. As  $\phi$  increases, the spatial pattern gradually flattens and, at the threshold  $\phi_1^*$ , the spatial pattern must connect to the uniform distribution. If we start from  $\bar{\mathbf{x}}$  and gradually *decrease*  $\phi$  to see the dispersion process in the reverse-reproduced way, at  $\phi_1^*$  the spatial pattern must deviate in the direction of the “formation” of a mono-centric configuration (Figure 6a). Proposition 6 predicts this bifurcation at  $\phi_1^*$ . To the left of the figure, the two city pattern also emerge (indicated by blue dashed curve). However, this configuration is always unstable.

## 5.2 How the network structure of social proximity affects the timing of dispersion?

We next illustrate that the timing of agglomeration varies with the structure of  $\mathbf{G}$ . If every region has the same interaction level to different regions, we can assume that  $\mathbf{G}$  takes the following form:

$$\mathbf{G}^\times \equiv \mathbf{G}^{\boxtimes} \Big|_{\psi'=\psi} = \begin{bmatrix} 1 & \psi & \psi & \psi \\ & 1 & \psi & \psi \\ & & 1 & \psi \\ \text{Sym.} & & & 1 \end{bmatrix}. \quad (5.11)$$

This setup is akin to equidistant geographical networks considered by, e.g., [Gaspar et al. \(2018, 2019\)](#). This economy can be thought as an “almost connected economy,” since the payoff in a region is invariant under the permutation of mobile workers in the other regions. That is, the exact distribution of workers over the other regions does not matter.

For this setting, we have  $\mathbf{z}^* = (1, 0, -1, 0)$ , in line with Section 5.1. The difference appears in the measure of interaction cost. Concretely, we have the following result.

**Proposition 7.** *Suppose  $n = 4$ . Assume  $\mathbf{D}$  in (5.1) and  $\mathbf{G} = \mathbf{G}^\times \equiv \mathbf{G}^{\boxtimes} \Big|_{\psi'=\psi}$ . Then,  $\omega^* = \Omega(\chi, \tilde{\lambda})$  and  $\mathbf{z}^* = (1, 0, -1, 0)$ , where  $\tilde{\lambda} \equiv \frac{1-\psi}{1+3\psi}$ . The uniform distribution  $\bar{\mathbf{x}}$  is linearly stable if and only if  $\omega^* < 0$ . When  $\bar{\mathbf{x}}$  become unstable, then a mono-centric pattern of the form  $\bar{\mathbf{x}} + \epsilon \mathbf{z}^*$  ( $\epsilon > 0$ ) emerges.*

The only difference from Proposition 6 is that we have

$$\tilde{\lambda} = \frac{1-\psi}{1+3\psi} \quad (5.12)$$

at the place of  $\lambda$ . Similar to Section 5.1,  $\tilde{\lambda}$  is the eigenvalue of  $\mathbf{G}^\times$  associated with  $\mathbf{z}^*$ . We see

$$\tilde{\lambda} = \frac{1-\psi}{1+3\psi} < \frac{1-\psi}{1+\psi} = \lambda, \quad (5.13)$$

which indicates that the average level of interaction cost in the economy is higher for the network  $\mathbf{G}^\square$  than for  $\mathbf{G}^{\boxtimes} \Big|_{\psi'=\psi}$ , which is intuitive.

As we note  $\Omega(\chi, \lambda)$  is increasing in  $\lambda$ , we have  $\Omega(\chi, \lambda) > \Omega(\chi, \tilde{\lambda})$  for any  $(\phi, \psi)$ . As a result,  $\bar{\mathbf{x}}$  is stable for a wider range of  $(\phi, \psi)$ . Figure 8 illustrates this observation. The solid and dashed curves indicate, respectively, critical pairs  $(\phi^*, \psi^*)$  for the matrices  $\mathbf{G}^\times$  and  $\mathbf{G}^\square$ . For each case,  $\bar{\mathbf{x}}$  is stable in the region above the threshold curve. The solid curve is always below the dashed curve, so that  $\bar{\mathbf{x}}$  is stable for a broader range of  $\phi$  and  $\psi$  when  $\mathbf{G}^\times$ . This is because, since the economy is socially more “connected” than  $\mathbf{G} = \mathbf{G}^\square$ , there is less incentive to form agglomeration. The result suggests that if social interactions is “closer” than geographical distance, it can promote dispersion of economic activities towards the peripheral regions.

## 5.3 How the network structure of social proximity affects the form of dispersion?

For both the cases considered in Sections 5.1 and 5.2, endogenous mechanisms induce a mono-centric agglomeration of the form Figure 6a. Endogenous spatial patterns can be, in fact, affected by interaction structure  $\mathbf{G}$ .

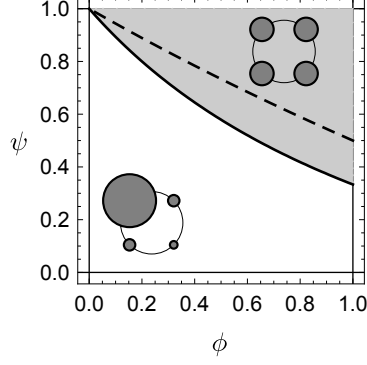


**Figure 8:** Stability of  $\bar{x}$  in the four-region economies with  $\mathbf{G}^\square$  and  $\mathbf{G}^\times = \mathbf{G}^\boxtimes|_{\psi'=\psi}$  ( $\sigma = 4$ ).

*Notes:* The black solid curve shows the critical pairs  $(\phi^*, \psi^*)$  at which  $\bar{x}$  becomes unstable for the case  $\mathbf{G} = \mathbf{G}^\boxtimes$  with  $\psi' = \psi$ . The dashed curve is that for the case  $\mathbf{G} = \mathbf{G}^\square$ . The uniform distribution  $\bar{x}$  is stable for the regions above these curves, where the gray regions correspond to  $\mathbf{G} = \mathbf{G}^\times$ . Observe that the solid curve stays below the dashed curve. That is,  $\bar{x}$  is stable for a wider range of  $(\phi, \psi)$  when the economy is more connected.

To see this section considers general  $\mathbf{G}^\boxtimes$  with arbitrary  $\psi' \in (0, 1)$  (with  $\psi' > 2\psi - 1$  to satisfy Assumption 1 (b)). We have the following characterization, which includes Propositions 6 and 7 as the special cases.

**Proposition 8.** *Suppose  $n = 4$ . Assume  $\mathbf{D}$  in (5.1) and  $\mathbf{G} = \mathbf{G}^\boxtimes$  with arbitrary  $\psi' \in (0, 1)$  such that  $\psi' > 2\psi - 1$ . Then, either  $\mathbf{z}^* = \mathbf{z}_1 \equiv (1, 0, -1, 0)$  or  $\mathbf{z}^* = \mathbf{z}_2 \equiv (1, -1, 1, -1)$ , and  $\omega^* = \max\{\omega_1, \omega_2\}$ , with  $\omega_k = \Omega(\chi_k, \lambda_k)$  where*

$$\chi_1 \equiv \chi, \quad \chi_2 \equiv \chi^2, \quad \lambda_1 \equiv \frac{1 - \psi'}{1 + 2\psi + \psi'} \in (0, 1), \quad \text{and} \quad \lambda_2 \equiv \frac{1 - 2\psi + \psi'}{1 + 2\psi + \psi'} \in (0, 1). \quad (5.14)$$

The uniform distribution  $\bar{x}$  is linearly stable if and only if  $\omega^* < 0$ . When  $\bar{x}$  become unstable, then either the mono-centric pattern  $\bar{x} + \epsilon \mathbf{z}_1$  if  $\omega^* = \omega_1$  or the duo-centric pattern  $\bar{x} + \epsilon \mathbf{z}_2$  emerges ( $\epsilon > 0$ ) if  $\omega^* = \omega_2$ .

Simply put, the duo-centric pattern (Figure 6b) can emerge, in contrast to Sections Section 5.1 and Section 5.2. The condition for the emergence of the duo-centric pattern is simply  $\omega^* = \omega_2$  (or  $\omega_2 > \omega_1$ ) when  $\bar{x}$  becomes unstable; the formation of the duo-centric pattern is more profitable for workers than the mono-centric pattern when  $\omega^* = \omega_2$ .

We highlight that  $\psi' > \psi$  is necessary for the duo-centric pattern to emerge. When  $\psi' > \psi$ , then region 1 is more socially “connected” to region 3 than to regions 2 or 4, and hence benefits more from social interactions with region 3 than with the others. Thus, with respect to  $\mathbf{G}$ , the regions at the antipodal locations in the circle are closer.

Similar to Sections 5.1 and 5.2,  $\lambda_1$  and  $\lambda_2$  are the eigenvalues of the row-normalized social proximity matrix. They are the indices of the inter-regional interaction costs when, respectively, the mono-centric and duo-centric configurations emerge. For instance, by employing the formula for  $\omega^*$ , we show that the uniform distribution can be stable for some  $\phi \in (0, 1)$  if and only if  $(\sigma - 1) \max\{\lambda_1, \lambda_2\} < 1$ . If inter-regional communication is almost prohibitive (i.e.,  $\psi \rightarrow 0$  and  $\psi' \rightarrow 0$ ), we have  $\lambda_1 \rightarrow 1$  and  $\lambda_2 \rightarrow 1$ . Thus,  $\bar{x}$  cannot be stable for such a case if  $\sigma > 2$ , which is obviously satisfied by the standard values of  $\sigma$  (Anderson and Van Wincoop, 2004). When  $\sigma$  is

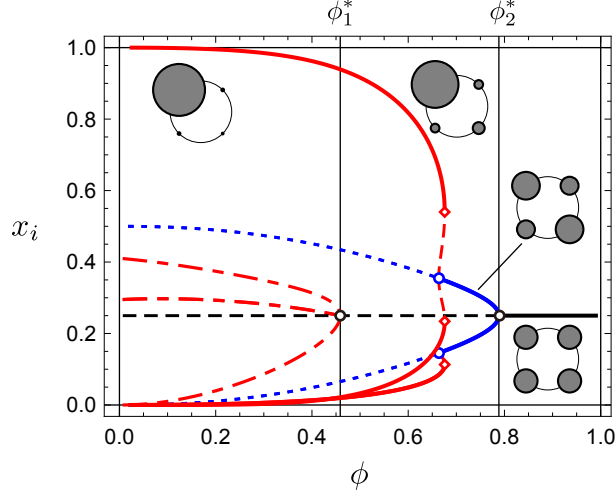


**Figure 9:** Bifurcation diagram for the four-region circular economy with social proximity matrix  $\mathbf{G}^\times$ .

Notes:  $\psi' = \psi^{1/2} > \psi$  with  $\psi^{1/2} = 0.65$  and  $\sigma = 4$ . The solid curves indicate stable equilibria, whereas the dashed or dotted curves indicate unstable ones. The red curves are mono-centric patterns, whereas the blue curve duo-centric pattern. The schematics by the solid curves show representative snapshots of associated stable spatial patterns.

sufficiently large, then workers are better off concentrating on a single region because differentiated goods are substitutes whereas inter-regional social interactions are too costly.

Figure 9 shows a numerical example in which  $\omega^* = \omega_2$ , so that stable duo-centric patterns emerge from  $\bar{x}$ . In line with Figure 7,  $\phi_1^*$  and  $\phi_2^*$  indicate, respectively, the level of  $\phi$  at which we have  $\omega_1 = 0$  and  $\omega_2 = 0$ . When  $\phi$  is small, a mono-centric distribution is stable (solid red curve), which is similar to Figure 7. As  $\phi$  increases, dispersion proceeds. The difference from Figure 7 is that region 3 attracts more workers than regions 2 and 4 in this process. For some range of  $\phi$ , there is a duo-centric concentration towards regions 1 and 3, but with asymmetry such that  $x_1 > x_3$ . At some point, the economy jumps to the symmetric two-peaked distribution (solid blue curve).<sup>3</sup> The two-peaked distribution connects smoothly to the uniform distribution at the critical value  $\phi_2^*$ . Proposition 8 predicts the bifurcation at  $\phi_2^*$ .

## 5.4 Super-regions

This section considers the case  $\mathbf{G} = \mathbf{G}^\square$  to investigate the role of hierarchical structure in the social proximity between regions as shown in Figure 5c. In the network  $\mathbf{G}^\square$ , the pairs of regions  $\{1, 2\}$  and  $\{3, 4\}$  can be interpreted as “super-regions.” Social interactions between the regions in the same super-region is freer than those between two regions in different super-regions, since we assume  $\psi' < \psi$  without loss of generality.

The following proposition shows that the stability of  $\bar{x}$  is determined by  $\psi'$  and the bifurcation from  $\bar{x}$  leads to the formation of a North–South pattern in Figure 6c.

**Proposition 9.** Suppose  $n = 4$ . Assume  $\mathbf{D}$  in (5.1) and  $\mathbf{G} = \mathbf{G}^\square$  with  $\psi' < \psi$ . Then,  $\omega^* = \Omega(\chi, \lambda')$  and

<sup>3</sup>This jump is encountered at a limit point for the mono-centric configuration (indicated by  $\diamond$ ), which is evidence of a saddle-node bifurcation.

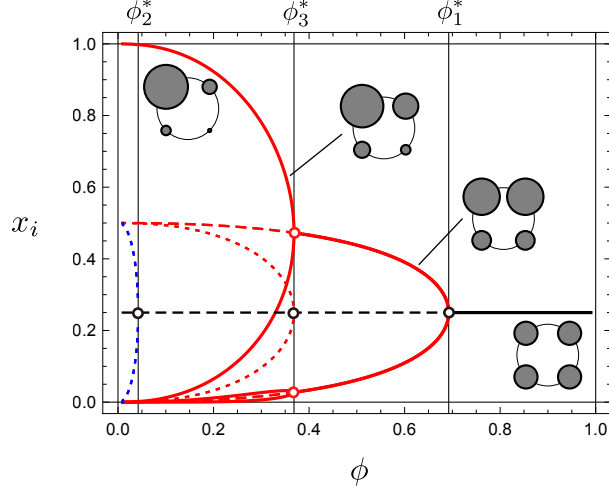


**Figure 10:** Bifurcation diagram for the four-region circular economy with social proximity matrix  $\mathbf{G}^{\square}$ .

Notes:  $\psi' = \psi^2 < \psi$  with  $\psi = 0.8$  and  $\sigma = 4$ . The solid curves indicate stable equilibria, whereas the dashed or dotted curves indicate unstable ones. The red curves are mono-centric patterns, whereas the blue curve duo-centric pattern. The schematics by the solid curves show representative snapshots of associated stable spatial patterns. For  $\phi \in (\phi_3^*, \phi_2^*)$ , the North–South pattern emerges. The economy exhibits a hierarchical structure of the North–South asymmetry and intra-regional asymmetry for the range  $\phi \in (0, \phi_3^*)$ .

$\mathbf{z}^* = (1, 1, -1, -1)$ , where  $\lambda' \equiv \frac{1-\psi'}{1+\psi'}$ . The uniform distribution  $\bar{\mathbf{x}}$  is linearly stable if and only if  $\omega^* < 0$ . When  $\bar{\mathbf{x}}$  become unstable, then a North–South pattern of the form  $\bar{\mathbf{x}} + \epsilon \mathbf{z}^*$  ( $\epsilon > 0$ ) emerges.

That is, the four-region economy with  $\mathbf{G} = \mathbf{G}^{\square}$  has quite similar properties as the two-region case. The intra-super-region interaction level,  $\psi$ , does not affect the bifurcation from  $\bar{\mathbf{x}}$  since  $\omega^*$  does not include it. Thus, we can regard each regional super-region as a “big” region, so we recover the two-region economy. There are two other possible migration patterns (i.e., the eigenvectors of  $\mathbf{V}$ ), but they are less profitable than North–South pattern  $\mathbf{z}^*$ . To be concrete, the possible migration patterns in this economy are

$$\mathbf{z}_1 = \mathbf{z}^* = (1, 1, -1, -1), \quad \mathbf{z}_2 = (1, -1, 1, -1), \quad \text{and} \quad \mathbf{z}_3 = (1, -1, -1, 1). \quad (5.15)$$

However, Appendix A.2 shows that the gains (i.e., the eigenvalues of  $\mathbf{V}$ ) associated with these patterns satisfy  $\omega^* = \omega_1 = \max\{\omega_1, \omega_2, \omega_3\}$  for all  $(\phi, \psi, \sigma)$ . The second migration pattern,  $\mathbf{z}_2$ , is the duo-centric pattern (Figure 6b), whereas the third an East–West pattern (90° rotation of the North–South pattern). The duo-centric pattern is less profitable than the East–West pattern, because, in the latter, the two big regions are close to each other and hence enjoy greater productivity than the former pattern. Similarly, the North–South pattern benefits from greater productivity than the East–West pattern, since the freeness of interaction between the two big regions are  $\psi$  in the former and  $\psi' < \psi$  in the latter. Thus, the most profitable deviation from  $\bar{\mathbf{x}}$  is North–South pattern  $\mathbf{z}_1$ .

Figure 10 shows a numerical example for this case. Each  $\phi_k^*$  indicates the level of  $\phi$  at which we have  $\omega_k = 0$  ( $k = 1, 2, 3$ ). When  $\phi$  is small, again a one-peaked distribution is stable (solid red curve). As  $\phi$  increases, dispersion proceeds. The difference from Figure 7 or Figure 9 is that

the North regions consistently attract more workers than the South. In the range  $\phi \in (0, \phi_3^*)$ , it is the process of gradual dispersion between regional super-regions, and the dispersion within the North. For the South, the process is ambiguous because there are two effects (within- and between-bloc) at work. For the range  $\phi \in (\phi_3^*, \phi_1^*)$  there is a steady North–South pattern, which connects smoothly to  $\bar{x}$  at the critical value  $\phi_1^*$  as predicted by Proposition 9. The process is understood as a hierarchical combination of the two-region story in Section 4.

We can show that the economy becomes closer to the baseline case in Section 5.1 as  $\psi' \rightarrow \psi$ . We have  $\phi_3^* \rightarrow \phi_1^*$  as  $\psi' \rightarrow \psi$  and then the bifurcation at  $\phi_1^*$  lead to the mono-centric pattern (Figure 6a) as in Section 5.1. In fact, when  $z_1$  and  $z_3$  become profitable at the same time, we see the migration pattern becomes  $\frac{1}{2}(z_1 + z_3) = (1, 0, -1, 0)$ , i.e., the mono-centric pattern.

## 6 Concluding remarks

This paper considered a bare-bones general equilibrium model with two proximity structures, one due to trade linkage and the other due to social linkage. The former is the standard linkage which many economic geography models in the literature focus on. In the symmetric two-region economy, we confirm that uniform dispersion is stable when the economy is integrated in terms of trade or social interactions. This is similar to the so-called “re-dispersion” in economic geography models with urban costs. In many-region settings, there are two first-order theoretical insights into the role of the additional proximity structure due to social interactions. First, it is demonstrated that the structure of the social proximity matrix affects the timing of endogenous agglomeration. Particularly, when the economy is socially more connected, there is less incentive for endogenous agglomeration. Second, the structure of social interaction network can, even when it is ex-ante symmetric, endogenously determine the overall form of the spatial distribution of workers across regions. Our examples, for instance, show that the number of major economic centers can depend on the interaction structure. When trade costs of goods become less relevant, the structure of social proximity emerges as a determinant of geographical distribution of workers.

The model considered in this paper obviously is a simple reduced-form; we build on the compromise that the social proximity structure is exogenously given. As discussed in Section 1, there are various interpretations for the “social proximity” matrix. The most interesting extension would be the endogenous determination of the social proximity structure in equilibrium. For such micro-founded models, our framework can be utilized to obtain coarse insights into the role of an additional network structure.

## A Proofs

This appendix collects the omitted proofs and derivations.

*Notations.* For vector-valued function  $f$ , we denote  $\mathbf{F}_x \equiv [\partial f_i / \partial x_j]$ . For vector  $x$ , we denote  $\hat{x} \equiv \text{diag}[x]$ .

### A.1 General properties

*Proof of Lemma 1.* We build on [Alvarez and Lucas \(2007\)](#). See also [Allen \(2019\)](#).

*Existence.* Let the excess demand function  $\Psi(\mathbf{w}) = (\Psi_i(\mathbf{w}))_{i \in \mathcal{N}}$  be defined as follows:

$$\Psi_i(\mathbf{w}) \equiv \frac{1}{w_i} \left( \sum_{k \in \mathcal{N}} \frac{a_i^{\sigma-1} w_i^{1-\sigma} \phi_{ik}}{\sum_{l \in \mathcal{N}} a_l^{\sigma-1} w_l^{1-\sigma} \phi_{lk}} w_k x_k - w_i x_i \right). \quad (\text{A.1})$$

Then, market wage is a solution for  $\Psi(\mathbf{w}) = \mathbf{0}$ . We see (i)  $\Psi(\cdot)$  is continuous, (ii)  $\Psi(\cdot)$  is homogeneous of degree zero, (iii)  $\mathbf{w}^\top \Psi(\mathbf{w}) = 0$  for any  $\mathbf{w}$  because of normalization of world income, and (iv)  $\Psi_i(\mathbf{w}) > -x_i > -1$ . Also, (v) for any sequence  $\{\mathbf{w}^n\}_{n=0}^\infty$  of strictly positive  $\mathbf{w}^n = (w_i^n)_{i \in \mathcal{N}}$  that converges to some  $\bar{\mathbf{w}} = (\bar{w}_i)_{i \in \mathcal{N}}$  such that  $\bar{w}_i = 0$  for some  $i^* \in \mathcal{N}$ , we have  $\max_{i \in \mathcal{N}} \Psi_i(\mathbf{w}^n) \rightarrow \infty$  as  $n \rightarrow \infty$ , because we see

$$\max_{i \in \mathcal{N}} \Psi_i(\mathbf{w}) = \max_{i \in \mathcal{N}} \sum_{k \in \mathcal{N}} \frac{a_i^{\sigma-1} w_i^{-\sigma} \phi_{ik}}{\sum_{l \in \mathcal{N}} a_l^{\sigma-1} w_l^{1-\sigma} \phi_{lk}} w_k x_k - \max_{i \in \mathcal{N}} x_i \quad (\text{A.2})$$

$$> \max_{i \in \mathcal{N}} \max_{j \in \mathcal{N}} \frac{a_i^{\sigma-1} w_i^{-\sigma} \phi_{ij}}{\sum_{l \in \mathcal{N}} a_l^{\sigma-1} w_l^{1-\sigma} \phi_{lj}} w_j x_j - 1 \quad (\text{A.3})$$

$$> \max_{i \in \mathcal{N}} \frac{a_i^{\sigma-1} \phi_{ij^*}}{\sum_{l \in \mathcal{N}} a_l^{\sigma-1} \phi_{lj^*}} w_{j^*} x_{j^*} \frac{w_i^{-\sigma}}{(\min_{k \in \mathcal{N}} w_k)^{1-\sigma}} - 1 \quad (\text{A.4})$$

$$> \max_{i \in \mathcal{N}} \frac{a_i^{\sigma-1} \phi_{ij^*}}{\sum_{l \in \mathcal{N}} a_l^{\sigma-1} \phi_{lj^*}} w_{j^*} x_{j^*} \frac{1}{\min_{k \in \mathcal{N}} w_k} - 1, \quad (\text{A.5})$$

where  $j^* \in \mathcal{N}$  is the regional index that achieves the second maximum in (A.3). The right hand side of the last display (A.5) goes to positive infinity because  $\min_{k \in \mathcal{N}} w_k^n \rightarrow \min_{k \in \mathcal{N}} \bar{w}_k = \bar{w}_{i^*} = 0$  as  $n \rightarrow \infty$  and the other component is positive. Therefore,  $\Psi(\mathbf{w})$  satisfies hypothesis (i)–(v) of [Mas-Colell et al. \(1995\)](#), Proposition 17.C.1 on p.585 and there is  $\mathbf{w}$  such that  $\Psi(\mathbf{w}) = \mathbf{0}$  and  $w_i > 0$  for all  $i \in \mathcal{N}$ .

*Uniqueness.* Note that  $\Psi(\cdot)$  has the *gross substitute property*. That is,

$$\frac{\partial \Psi_i(\mathbf{w})}{\partial w_j} = \frac{1}{w_i} \left( m_{ij} x_j + (\sigma - 1) \sum_{k \in \mathcal{N}} m_{ik} m_{jk} w_k x_k \frac{1}{w_j} \right) > 0 \quad (\text{A.6})$$

for any  $i \neq j$ , where we let

$$m_{ij} = \frac{a_i^{\sigma-1} w_i^{1-\sigma} \phi_{ij}}{\sum_{l \in \mathcal{N}} a_l^{\sigma-1} w_l^{1-\sigma} \phi_{lj}}. \quad (\text{A.7})$$

Note that the first term in the parenthesis is nonnegative and the second term is positive. Hence, by Proposition 17.F.3 of [Mas-Colell et al. \(1995\)](#), there exists unique  $\mathbf{w}$  up to scale such that  $\Psi(\mathbf{w}) = \mathbf{0}$ . Thus, there is unique  $\mathbf{w}$  that satisfy  $\Psi(\mathbf{w}) = \mathbf{0}$  and  $\sum_{i \in \mathcal{N}} w_i x_i = 1$ .

*Diverge when  $x_i \rightarrow 0$ .* By rewriting the condition  $\Psi_i(\mathbf{x}) = 0$ , we see

$$w_i^\sigma = \frac{1}{x_i} \sum_{k \in \mathcal{N}} \frac{a_i^{\sigma-1} \phi_{ik}}{\sum_{l \in \mathcal{N}} a_l^{\sigma-1} w_l^{1-\sigma} \phi_{lk}} w_k x_k > \frac{1}{x_i} \min_{k \in \mathcal{N}} \frac{a_i^{\sigma-1} \phi_{ik}}{\sum_{l \in \mathcal{N}} a_l^{\sigma-1} w_l^{1-\sigma} \phi_{lk}} \sum_{j \in \mathcal{K}} w_j x_j \quad (\text{A.8})$$

$$> \frac{1}{x_i} \min_{k \in \mathcal{N}} \frac{a_i^{\sigma-1} \phi_{ik}}{\sum_{l \in \mathcal{N}} a_l^{\sigma-1} \phi_{lk}} \min_{l \in \mathcal{N}} w_l^{\sigma-1} = C_1 C_2 x_i^{-1}, \quad (\text{A.9})$$

where  $C_1 \equiv \min_{k \in \mathcal{N}} a_i^{\sigma-1} \phi_{ik} \left( \sum_{l \in \mathcal{N}} a_l^{\sigma-1} \phi_{lk} \right)^{-1} > 0$  and  $C_2 \equiv \min_{l \in \mathcal{N}} w_l^{\sigma-1} > 0$ , i.e.,  $w_i \rightarrow \infty$  as  $x_i \rightarrow 0$ .  $\square$

*Proof of Proposition 1.* In general, a spatial equilibrium is a spatial distribution  $x \in \mathcal{X}$  such that the following Nash equilibrium condition is met for the location choice of workers:

$$\begin{cases} v^* = v_i(x) \text{ for all regions } i \in \mathcal{N} \text{ with } x_i > 0, \\ v^* \geq v_i(x) \text{ for any region } i \in \mathcal{N} \text{ with } x_i = 0, \end{cases} \quad (\text{A.10})$$

where  $v^*$  is an equilibrium payoff. The following *variational inequality problem* is equivalent to (A.10):

$$\text{Find } x \in \mathcal{X} \text{ such that } v(x)^\top (y - x) \leq 0 \text{ for all } y \in \mathcal{X}. \quad (\text{VIP})$$

Every region is necessarily populated at any spatial equilibrium when  $\mathbf{D}$  and  $\mathbf{G}$  are positive (i.e.,  $\phi_{ij} > 0$  and  $\psi_{ij} > 0$  for all  $i, j \in \mathcal{N}$ ). First,  $a_i(x) > 0$  for all  $i \in \mathcal{N}$  at any  $x \in \mathcal{X}$  when  $\mathbf{G}$  is positive. Next, we see

$$v_i^{\sigma-1} = w_i^{\sigma-1} \sum_{j \in \mathcal{N}} a_j^{\sigma-1} w_j^{1-\sigma} \phi_{ji} > w_i^{\sigma-1} \sum_{j \neq i} a_j^{\sigma-1} w_j^{1-\sigma} \phi_{ji} > C_3 C_4 w_i^{\sigma-1} \quad (\text{A.11})$$

where  $C_3 \equiv \min_{j \neq i} a_j^{\sigma-1} \phi_{ij} > 0$  (by positivity of  $\phi_{ij}$ ) and  $C_4 \equiv \min_{j \neq i} w_j^{1-\sigma} > 0$  (by positivity of  $w_i$  shown by Lemma 1). Note also that  $C_4$  is bounded for all positive  $x$ .

By (A.11) and (A.9), for any sequence of positive spatial patterns  $\{x^n\}_{n=1}^\infty$  that converges to a spatial distribution such that  $x_i = 0$ ,  $w_i(x^n)$  and  $v_i(x^n)$  both diverge to positive infinity as  $n \rightarrow \infty$ . On the other hand, by Lemma 1,  $w$  is uniquely given if we focus on the regions with positive population  $\mathcal{N}_+ \equiv \{k \in \mathcal{N} \mid x_k > 0\}$  by letting  $w_i := \infty$  and  $w_i x_i := 0$  for all  $i \in \mathcal{N}_0 \equiv \{k \in \mathcal{N} \mid x_k = 0\}$ . Then,  $v_i(x)$  is finite for all  $i \in \mathcal{N}_+$ , while  $v_i(x)$  is infinitely large for any  $i \in \mathcal{N}_0$ . Since such spatial distribution cannot be a spatial equilibrium, every region is necessarily populated in equilibrium. Thus, the equilibrium condition (A.10) in fact reduces to the equality:  $v_i(x) = v_j(x)$  for all  $i, j \in \mathcal{N}$ .

Consider the following variational inequality problem, which is a “restricted” version of (VIP):

$$\text{Find } x \in \mathcal{X}_\epsilon \text{ such that } v(x)^\top (y - x) \leq 0 \text{ for all } y \in \mathcal{X}_\epsilon, \quad (\text{VIP}_\epsilon)$$

where  $\mathcal{X}_\epsilon \equiv \{x \in \mathcal{X} \mid x_i > \epsilon \forall i \in \mathcal{N}\}$  for some  $\epsilon > 0$ . Since  $v$  is differentiable and thus continuous on  $\mathcal{X}_\epsilon$ , and  $\mathcal{X}_\epsilon$  is compact and convex, by Corollary 2.2.5 of Facchinei and Pang (2003), the set of solutions for (VIP $_\epsilon$ ) is nonempty and compact for any choice of  $\epsilon > 0$ . There is some  $\epsilon > 0$  for which all solutions for (VIP $_\epsilon$ ) are in the (relative) interior of  $\mathcal{X}_\epsilon$  because  $v_i(x)$  is continuous in  $x$  and diverges when  $x_i \rightarrow 0$ . Because any interior solution for (VIP $_\epsilon$ ) must satisfy  $v_i(x) = v_j(x)$  for all  $i, j \in \mathcal{N}$ , they are spatial equilibria.  $\square$

*Proof of Proposition 2.* Suppose  $\phi_{ij} = 1$  and  $\psi_{ij} = 1$  for all  $i, j \in \mathcal{N}$ . Then,  $a_i(x) = 1$  and

$$m_{ij} = \frac{w_i^{1-\sigma} \phi_{ij}}{\sum_{l \in \mathcal{N}} w_l^{1-\sigma} \phi_{lj}} = m_i \equiv \frac{w_i^{1-\sigma}}{\sum_{l \in \mathcal{N}} w_l^{1-\sigma}} \in (0, 1), \quad (\text{A.12})$$

This implies that

$$w_i x_i = \sum_{j \in \mathcal{N}} m_{ij} w_j x_j = m_i \sum_{j \in \mathcal{N}} w_j x_j = m_i. \quad (\text{A.13})$$

Also, we see

$$v_i(x) = \frac{w_i}{P_i} = \left( \frac{w_i^{1-\sigma}}{\sum_{j \in \mathcal{N}} w_j^{1-\sigma}} \right)^{\frac{1}{1-\sigma}} = m_i^{\frac{1}{1-\sigma}}. \quad (\text{A.14})$$

Since all regions are populated in equilibrium, we have  $m_i = \bar{m} \in (0, 1)$  for all  $i \in \mathcal{N}$  for  $x$  to be an equilibrium. By (A.12),  $w_i = \bar{w} > 0$  for all  $i \in \mathcal{N}$ . From (A.13), we conclude  $x_i = \frac{\bar{m}}{\bar{w}} = \bar{x} = \frac{1}{n}$  for all  $i \in \mathcal{N}$ . That is,  $\bar{x}$  is the unique equilibrium. The stability of  $\bar{x}$  can be shown by knowing  $\mathbf{V}_x$  is negative definite at  $x = \bar{x}$ . In fact,  $\mathbf{V}_x$  is symmetric at  $\bar{x}$  and all of its relevant eigenvalues take the same value  $-\sigma^{-1} < 0$ . This can be shown by letting  $\chi_k \rightarrow 0$  and  $\lambda_k \rightarrow 0$  in Fact A.1 shown below.  $\square$

*Proof of Proposition 3.* When  $\phi_{ij} = 0$  and  $\psi_{ij} = 0$  so that inter-regional trade and social interactions are prohibitive, we have  $a_i = x_i$  for all  $i \in \mathcal{N}$ . Further, the market equilibrium conditions reduce to:

$$w_i x_i = x_i^{\sigma-1} w_i^{1-\sigma} w_i x_i, \quad (\text{A.15})$$

thereby  $w_i = x_i$ . Thus,  $P_i = (x_i^{\sigma-1} x_i^{1-\sigma})^{1/(1-\sigma)} = 1$  and  $v_i(\mathbf{x}) = x_i$ . Therefore, any spatial distribution in which the populated regions have the same population is an equilibrium when  $\phi_{ij}$  and  $\psi_{ij}$  vanish for all  $i \neq j$ . However, all such equilibria with more than one populated regions cannot be stable under natural dynamics since any migration between populated regions induce relative payoff advantages. Therefore, the economy ends up with a complete mono-centric agglomeration when  $\phi_{ij} = 0$  and  $\psi_{ij} = 0$  for all  $i \neq j$ . Because equilibria is continuous in  $\phi_{ij}$  and  $\psi_{ij}$ , we conclude the assertion.  $\square$

## A.2 Stability of the uniform distribution

We first give general characterization of stability of  $\bar{\mathbf{x}}$  for both  $n = 2$  and  $n = 4$ . Our approach build on [Akamatsu et al. \(2012\)](#), which is recently synthesized by [Akamatsu et al. \(2019\)](#).

For any  $\mathbf{D} > 0$  and  $\mathbf{G} > 0$ , we compute that

$$\mathbf{V}_x = \hat{v}(\mathbf{x}) \left( \mathbf{M}^\top \hat{\mathbf{a}}^{-1} \mathbf{A}_x + (\mathbf{I} - \mathbf{M}^\top) \hat{w}^{-1} \mathbf{W}_x \right) \quad (\text{A.16})$$

where  $\mathbf{M} = [m_{ij}]$  with  $m_{ij}$  defined by (A.7). The Jacobian matrix of wage with respect to spatial distribution  $\mathbf{x}$ ,  $\mathbf{W}_x$ , is given by the implicit function theorem regarding the short-run market equilibrium condition:

$$z_i(\mathbf{x}, \mathbf{w}) \equiv w_i x_i - \sum_{k \in \mathcal{N}} m_{ik} w_k x_k = 0 \quad (\text{A.17})$$

as  $\mathbf{W}_x = -\mathbf{Z}_w^{-1} \mathbf{Z}_x$ . We compute

$$\mathbf{Z}_w = \left( \sigma \hat{\mathbf{y}} - (\sigma - 1) \mathbf{M} \hat{\mathbf{y}} \mathbf{M}^\top - \mathbf{M} \hat{\mathbf{y}} \right) \hat{w}^{-1}, \quad (\text{A.18})$$

$$\mathbf{Z}_x = \left( \hat{\mathbf{y}} - (\sigma - 1) \left( \hat{\mathbf{y}} - \mathbf{M} \hat{\mathbf{y}} \mathbf{M}^\top \right) \hat{\mathbf{a}}^{-1} \mathbf{A}_x \hat{\mathbf{x}} - \mathbf{M} \hat{\mathbf{y}} \right) \hat{\mathbf{x}}^{-1} \quad (\text{A.19})$$

where  $\mathbf{y} = (w_i x_i)_{i \in \mathcal{N}}$ . We note  $\mathbf{A}_x = \mathbf{G}$ .

Consider a  $n$ -region economy ( $n \geq 2$ ). Suppose uniform distribution  $\bar{\mathbf{x}} = (\bar{x}, \bar{x}, \dots, \bar{x})$  with  $\bar{x} = \frac{1}{n}$ . Let  $\bar{\mathbf{D}}$  and  $\bar{\mathbf{G}}$  be the row-normalized versions of  $\mathbf{D}$  and  $\mathbf{G}$ . We have  $\mathbf{M} = \bar{\mathbf{D}}$  and  $\hat{\mathbf{a}}^{-1} \mathbf{A}_x = \bar{\mathbf{G}}$  at  $\bar{\mathbf{x}}$ . We impose the following assumption on  $\bar{\mathbf{D}}$  and  $\bar{\mathbf{G}}$ , which is satisfied by our examples in Sections 4 and 5.

**Assumption A.3.** Both  $\bar{\mathbf{D}}$  and  $\bar{\mathbf{G}}$  are either circulants or block circulants with circulant blocks (BCCBs).

Under the assumption,  $\bar{\mathbf{D}}$  and  $\bar{\mathbf{G}}$  commute. In turn, we evaluate as follows:

$$\mathbf{W}_x = -\frac{\bar{w}}{\bar{x}} (\sigma \mathbf{I} + (\sigma - 1) \bar{\mathbf{D}})^{-1} (-\mathbf{I} + (\sigma - 1) (\mathbf{I} + \bar{\mathbf{D}}) \bar{\mathbf{G}}) \quad (\text{A.20})$$

$$\mathbf{V}_x = \frac{\bar{v}}{\bar{x}} (\sigma \mathbf{I} + (\sigma - 1) \bar{\mathbf{D}})^{-1} (-\mathbf{I} - \bar{\mathbf{D}}) + ((\sigma - 1) \mathbf{I} + \sigma \bar{\mathbf{D}}) \bar{\mathbf{G}}, \quad (\text{A.21})$$

where  $\bar{v}$  is the uniform level of payoff at  $\bar{\mathbf{x}}$ . We let  $\mathbf{V} = \frac{\bar{x}}{\bar{v}} \mathbf{V}_x$ . By assumption,  $\mathbf{V}$  is real and symmetric.

When  $\mathbf{V}$  is negative definite with respect to  $T\mathcal{X} = \{\mathbf{z} \in \mathbb{R}^n \mid \sum_{i \in \mathcal{N}} z_i = 0\}$ ,  $\bar{\mathbf{x}}$  is *evolutionary stable state* (see [Sandholm, 2010](#), Observation 8.3.11). Then,  $\bar{\mathbf{x}}$  is stable under all admissible dynamics. Since  $\mathbf{V}$  is symmetric, it is negative definite if and only if all of its eigenvalues with respect to  $T\mathcal{X}$  is negative.

We have the following fact (see, e.g., [Horn and Johnson, 2012](#)).

**Fact A.1.** Under Assumption A.3, the eigenvalues of  $\mathbf{V}$  are given by:

$$\omega_k = \Omega(\chi_k, \lambda_k) \equiv \frac{\Omega^\sharp(\chi_k, \lambda_k)}{\Omega^b(\chi_k)} \quad \forall k, \quad (\text{A.22})$$

where  $\chi_k$  and  $\lambda_k$  are, respectively, the  $k$ th eigenvalues of  $\bar{\mathbf{D}}$  and  $\bar{\mathbf{G}}$ , and we define

$$\Omega^\sharp(\chi, \lambda) \equiv -(1 - \chi) + ((\sigma - 1) + \sigma\chi) \lambda, \quad (\text{A.23})$$

$$\Omega^\flat(\chi) \equiv \sigma + (\sigma - 1)\chi. \quad (\text{A.24})$$

The three matrices  $\mathbf{V}$ ,  $\bar{\mathbf{D}}$ , and  $\bar{\mathbf{G}}$  share the same set of eigenvectors. One eigenvector is  $\mathbf{1} = (1, 1, \dots, 1)$  and is orthogonal to  $T\mathcal{X}$ . The other eigenvectors  $\{\mathbf{z}_k\}$  span  $T\mathcal{X}$  and each satisfies  $\mathbf{z}_k^\top \mathbf{1} = 0$ .  $\diamond$

The formula (A.24) is simply the translation of the matrix relationship (A.21) into an eigenvalue relationship, which made possible by the properties of circulant matrices (or BCCBs). In effect, the stability of  $\bar{x}$  is determined by eigenvalues  $\{\omega_k\}$  that corresponds to the eigenvectors other than  $\mathbf{1}$ .

It is a standard fact in dynamical systems theory that when some eigenvalues  $\omega_k$  switches from negative to positive, then the state is pushed towards the direction of the associated eigenvector (see, e.g., [Kuznetsov, 2004](#), Chapter 5). (The ‘‘critical’’ eigenvector is tangent to the unstable manifold emanating from  $\bar{x}$ .) When

$$\omega_{\max} \equiv \max_k \{\omega_k\} \quad (\text{A.25})$$

turns its sign from negative to positive, then the spatial distribution is perturbed towards the direction of the associated eigenvector  $\mathbf{z}_{k^*}$ , where  $k^* \equiv \arg \max_k \{\omega_k\}$ . Intuitively, each eigenvalues  $\omega_k$  is the gain for migrants when they collaterally migrate toward the direction of the associated eigenvector.

To be more explicit, we proceed as follows. Consider a general perturbation of  $\bar{x}$  such that  $\mathbf{x} = \bar{x} + \mathbf{z}$ , where  $\mathbf{z}^\top \mathbf{1} = 0$ . Rewrite  $\mathbf{z}$  as

$$\mathbf{z} = \sum_{k \in \mathcal{K}} c_k \mathbf{z}_k, \quad (\text{A.26})$$

where  $\mathcal{K} \equiv \{1, 2, 3\}$  and  $\{\mathbf{z}_k\}_{k \in \mathcal{K}}$  are the eigenvectors of  $\mathbf{V}$  such that  $\mathbf{z}_k^\top \mathbf{1} = 0$  and  $\|\mathbf{z}_k\|^2 = \mathbf{z}_k^\top \mathbf{z}_k = 1$ . For our examples of  $\bar{\mathbf{D}}$  and  $\bar{\mathbf{G}}$ , matrix  $\mathbf{V}$  is symmetric. Thus, the eigendecomposition of  $\mathbf{V}$  is given by:

$$\mathbf{V} = \omega_0 \mathbf{1}\mathbf{1}^\top + \sum_{k \in \mathcal{K}} \omega_k \mathbf{z}_k \mathbf{z}_k^\top, \quad (\text{A.27})$$

where  $\omega_k$  is the eigenvalue associated with  $\mathbf{z}_k$ , with  $\mathbf{z}_0 = \mathbf{1} = (1, 1, 1, 1)$ . By plugging (A.26) and (A.27) into (5.4), we can evaluate  $\bar{\omega}$  as:

$$\bar{\omega} = \mathbf{z}^\top \mathbf{V} \mathbf{z} = \sum_{k \in \mathcal{K}} \omega_k c_k^2. \quad (\text{A.28})$$

It shows that  $\bar{\omega}$  is maximized by  $\mathbf{z} = \mathbf{z}_{k^*}$ , where  $k^* = \arg \max_{k \in \mathcal{K}} \omega_k$ :

$$\omega_{\max} \equiv \max_{\mathbf{z}: \|\mathbf{z}\|=1} \bar{\omega} = \omega_{k^*}, \quad (\text{A.29})$$

where we assume  $\|\mathbf{z}\|^2 = \mathbf{z}^\top \mathbf{z} = \sum_{k \in \mathcal{K}} c_k^2 = 1$ . The uniform distribution is stable when

$$\omega_{\max} = \omega_{k^*} = \max_{k \in \mathcal{K}} \{\omega_k\} < 0. \quad (\text{A.30})$$

The relevant eigenvalues  $\{\omega_k\}$  are given by the formula (A.22). They depend on the properties of  $\bar{\mathbf{D}}$  and  $\bar{\mathbf{G}}$  through  $\{\chi_k\}$  and  $\{\lambda_k\}$ . From (A.22), the stability of  $\bar{x}$  switches when:

$$\max_k \left\{ \Omega^\sharp(\chi_k, \lambda_k) \right\} \quad (\text{A.31})$$

changes its sign from negative to positive, since we have  $\Omega^\flat(\chi_k) > 0$  for all examples considered in this paper. In the following, we provide the proofs for each examples in Sections 4 and 5.

*Proof of Proposition 4.* When  $n = 2$ , both  $\bar{\mathbf{D}}$  and  $\bar{\mathbf{G}}$  are circulants.  $\mathbf{V}$  can be diagonalized by the following discrete Fourier transformation (DFT) matrix:

$$\mathbf{Z}_2 \equiv \frac{1}{\sqrt{2}} \begin{bmatrix} 1 & 1 \\ 1 & -1 \end{bmatrix}, \quad (\text{A.32})$$

where each column vector is an eigenvector (migration pattern) of  $\mathbf{V}$ . The relevant eigenvector is  $z = (1, -1)$ , because  $\mathbf{1} = (1, 1)$  violates the conservation of workers' population. The eigenvalue of  $\bar{\mathbf{D}}$  and  $\bar{\mathbf{G}}$  associated with  $z$  are, respectively, given by

$$\chi = \frac{1-\phi}{1+\phi} \quad \text{and} \quad \lambda = \frac{1-\psi}{1+\psi}. \quad (\text{A.33})$$

That  $\omega = \Omega(\chi, \lambda) < 0$  implies  $\mathbf{V}$  is negative definite with respect to  $T\mathcal{X}$  and in turn the stability of  $\bar{x}$ .  $\square$

*Proof of Propositions 6, 7, and 8.* Both  $\bar{\mathbf{D}}$  and  $\bar{\mathbf{G}}$  are circulant matrices. The social proximity matrices considered in these propositions are special cases of general specification  $\mathbf{G}^{\boxtimes}$ . For these examples,  $\mathbf{V}$  is diagonalized by the following DFT matrix:

$$\mathbf{Z}_4 \equiv \frac{1}{2} \begin{bmatrix} 1 & 1 & 1 & 1 \\ 1 & i & -1 & -i \\ 1 & -1 & 1 & -1 \\ 1 & -i & -1 & i \end{bmatrix} \quad (\text{A.34})$$

where  $i$  is the imaginary unit ( $i^2 = -1$ ). The relevant (real) eigenvectors are obtained by combining the columns of  $\mathbf{Z}_4$  as follows:  $z_1 = (1, 0, -1, 0)$ ,  $z_2 = (1, -1, 1, -1)$ , and  $z_3 = (0, 1, 0, -1)$ , where we omit the normalizing constants for simplicity.  $z_1$  and  $z_3$  share the same eigenvalues. This is because  $z_1$  and  $z_3$  represent the same spatial configuration (the economy is symmetric under rotation).

The eigenvalues of  $\bar{\mathbf{D}}$  associated with  $z_1$  and  $z_2$  are, respectively,

$$\chi_1 = \frac{1-\phi}{1+\phi} \quad \text{and} \quad \chi_2 = \left( \frac{1-\phi}{1+\phi} \right)^2. \quad (\text{A.35})$$

Also, the eigenvalues of  $\bar{\mathbf{G}}^{\boxtimes}$  associated with  $z_1$  and  $z_2$  are, respectively,

$$\lambda_1 = \frac{1-\psi'}{1+2\psi+\psi'} \quad \text{and} \quad \lambda_2 = \frac{1-2\psi+\psi'}{1+2\psi+\psi'}. \quad (\text{A.36})$$

The uniform distribution is stable when  $\omega_k = \Omega(\chi_k, \lambda_k) < 0$  for both  $k = 1$  and  $k = 2$ .  $\psi' = \psi^2$  implies Proposition 6, whereas  $\psi' = \psi$  implies Proposition 7. For both the two cases, we have  $\omega_1 = \max\{\omega_1, \omega_2\}$ , thereby mono-centric pattern  $z_1$  (Figure 6a) emerges from  $\bar{x}$ . Proposition 8 follows because  $k = \arg \max_k \{\omega_1, \omega_2\}$  depends on the values of  $(\phi, \psi, \psi')$ . Particularly,  $\psi' > \psi$  is necessary for  $\omega_2 > \omega_1$ .  $\square$

*Proof of Proposition 9.* Both  $\mathbf{D}$  and  $\mathbf{G}^{\boxplus}$  are  $2 \times 2$  BCCBs. Then,  $\mathbf{V}$  is diagonalized by the following two-dimensional DFT matrix:

$$\mathbf{Z}_2 \otimes \mathbf{Z}_2 = \frac{1}{\sqrt{2}} \begin{bmatrix} \mathbf{Z}_2 & \mathbf{Z}_2 \\ \mathbf{Z}_2 & -\mathbf{Z}_2 \end{bmatrix} = \frac{1}{2} \begin{bmatrix} 1 & 1 & 1 & 1 \\ 1 & -1 & 1 & -1 \\ 1 & 1 & -1 & -1 \\ 1 & -1 & -1 & 1 \end{bmatrix} \quad (\text{A.37})$$

The relevant eigenvectors are  $z_1 = (1, 1, -1, -1)$ ,  $z_2 = (1, -1, 1, -1)$ , and  $z_3 = (1, -1, -1, 1)$ .  $z_1$  is the North-South pattern in Figure 6c, whereas  $z_3$  is its rotation (the "East-West" pattern).  $z_2$  is the duo-centric pattern.

The eigenvalues of  $\bar{\mathbf{D}}$  associated with  $z_1$ ,  $z_2$ , and  $z_3$  are, respectively,

$$\chi_1 = \frac{1-\phi}{1+\phi}, \quad \chi_2 = \left( \frac{1-\phi}{1+\phi} \right)^2, \quad \text{and} \quad \chi_3 = \frac{1-\phi}{1+\phi}. \quad (\text{A.38})$$

Similarly, the eigenvalues of  $\bar{\mathbf{G}}^{\boxplus}$  associated with  $z_1$ ,  $z_2$ , and  $z_3$  are, respectively,

$$\lambda_1 = \frac{1-\psi'}{1+\psi'}, \quad \lambda_2 = \left( \frac{1-\psi'}{1+\psi'} \right) \left( \frac{1-\psi}{1+\psi} \right), \quad \text{and} \quad \lambda_3 = \frac{1-\psi}{1+\psi}. \quad (\text{A.39})$$

We have  $\omega_k = \Omega(\chi_k, \lambda_k) = 0$  if and only if  $\omega_k^\# \equiv \Omega^\#(\chi_k, \lambda_k) = 0$ . Since  $\lambda_1 > \lambda_3 > \lambda_2$  and  $\chi_1 = \chi_3 > \chi_2$ , we see  $\omega_1^\# = \max_k \{\omega_k^\#\}$ . Thus, North–South pattern  $z_1$  (Figure 6c) must emerge when  $\bar{x}$  become unstable.  $\square$

### A.3 Pitchfork bifurcation from the uniform distribution

*Proof of Proposition 5.* When  $n = 2$ , the uniform distribution  $\bar{x} = (\bar{x}, \bar{x})$  can be viewed as steady-state solution  $y = 0$  for the following one-dimensional autonomous system:

$$\dot{y} = \Delta v(y, \mu) \equiv v_1(x(y)) - v_2(x(y)), \quad (\text{A.40})$$

where we choose  $y \in \mathcal{Y} \equiv (-\bar{x}, \bar{x})$  and let  $x(y) = (x_1(y), x_2(y)) \equiv (\bar{x} + y, \bar{x} - y)$ . The bifurcation parameter  $\mu$  indicates either  $\phi$  or  $\psi$ . Under admissible dynamics, the bifurcation diagram become smoothly equivalent to the system (A.40). In the following, prime (') denotes differentiation with respect to one-dimensional variable  $y$ .

In general, the system (A.40) undergoes pitchfork bifurcation at  $(y, \mu) = (0, \mu^*)$  when  $\Delta v(y, \mu)$  is odd in  $y$  and the following conditions are met (see, e.g., Wiggins, 2003, Section 20.1E):

$$\Delta v'(0, \mu^*) = 0, \quad \Delta v''(0, \mu^*) = 0, \quad \Delta v'''(0, \mu^*) \neq 0, \quad \frac{\partial \Delta v(0, \mu^*)}{\partial \mu} = 0, \quad \text{and} \quad \frac{\partial \Delta v'(0, \mu^*)}{\partial \mu} \neq 0. \quad (\text{A.41})$$

We see  $\Delta v$  is odd:  $\Delta v(-y, \mu) = -\Delta v(y, \mu)$ . The fourth condition also follows, for  $\Delta v(0, \mu) = 0$  for all  $\mu$ .

The first condition (*nonhyperbolicity*) ensures that  $\mu = \mu^*$  is the bifurcation point:

$$\Delta v'(0, \mu^*) = \left( \frac{\partial v_1(\bar{x})}{\partial x_1} \frac{\partial x_1(0)}{\partial y} + \frac{\partial v_1(\bar{x})}{\partial x_2} \frac{\partial x_2(0)}{\partial y} \right) - \left( \frac{\partial v_2(\bar{x})}{\partial x_1} \frac{\partial x_1(0)}{\partial y} + \frac{\partial v_2(\bar{x})}{\partial x_2} \frac{\partial x_2(0)}{\partial y} \right) \quad (\text{A.42})$$

$$= \left( \frac{\partial v_1(\bar{x})}{\partial x_1} - \frac{\partial v_1(\bar{x})}{\partial x_2} \right) - \left( \frac{\partial v_2(\bar{x})}{\partial x_1} - \frac{\partial v_2(\bar{x})}{\partial x_2} \right) = \mathbf{z}^\top \mathbf{V}_x \mathbf{z} = \frac{2\bar{v}}{\bar{x}} \omega(\mu^*) \quad (\text{A.43})$$

where  $\mathbf{z} = (1, -1)$  and we recall  $\omega$  is the eigenvalue of  $\mathbf{V} = \frac{\bar{x}}{\bar{v}} \mathbf{V}_x$  associated with  $\mathbf{z}$ . The bifurcation point regarding freeness parameters  $(\phi, \psi)$  is the solution for  $\omega = 0$  and we have  $\Delta v'(0, \mu) = 0$ . For  $\omega(\phi, \psi) = 0$  (or  $\Omega^\#(\chi(\phi), \lambda(\psi)) = 0$ ) to admit solution such that  $(\chi, \lambda) \in (0, 1) \times (0, 1)$ , we need

$$\lambda^* \equiv \frac{1 - \chi}{(\sigma - 1) + \sigma \chi} \in (0, 1) \quad \forall \chi \in (0, 1), \quad (\text{A.44})$$

or, equivalently, either  $\sigma > 2$ , or  $\sigma \in (1, 2]$  and  $\chi \in (\frac{2-\sigma}{\sigma+1}, 1)$ . We assume either of these below.

From (A.43), we see

$$\frac{\partial \Delta v'(0, \mu^*)}{\partial \mu} = \frac{2}{\bar{x}} \left( \frac{\partial \bar{v}}{\partial \mu} \omega(\mu^*) + \bar{v} \frac{\partial \omega(\mu^*)}{\partial \mu} \right) = \frac{2\bar{v}}{\bar{x}} \frac{\partial \omega}{\partial \mu} \quad (\text{A.45})$$

by noting that  $\omega(\mu^*) = 0$ . With (A.22), we show the fifth condition in (A.41):

$$\frac{\partial \Delta v'(0, \mu^*)}{\partial \phi} = \frac{2\bar{v}}{\bar{x}} \frac{\partial \omega}{\partial \chi} \frac{\partial \chi}{\partial \phi} = -\frac{2}{\bar{x}} \cdot \frac{(1 + \lambda)(2\sigma - 1)}{(\sigma + (\sigma - 1)\lambda)^2} \cdot \frac{2}{(1 + \phi)^2} < 0, \quad (\text{A.46})$$

$$\frac{\partial \Delta v'(0, \mu^*)}{\partial \psi} = \frac{2\bar{v}}{\bar{x}} \frac{\partial \omega}{\partial \lambda} \frac{\partial \lambda}{\partial \psi} = -\frac{2}{\bar{x}} \cdot \frac{(\sigma - 1) + \sigma \chi}{\sigma + (\sigma - 1)\lambda} \cdot \frac{2}{(1 + \psi)^2} < 0. \quad (\text{A.47})$$

For  $\Delta v''(0, \mu^*)$  and  $\Delta v'''(0, \mu^*)$ , we resort to more explicit computations. Let  $w_1 : \mathcal{Y} \rightarrow \mathbb{R}_+$  and  $w_2 : \mathcal{Y} \rightarrow \mathbb{R}_+$  denote, respectively, the nominal wages of regions 1 and 2 as functions of  $y \in \mathcal{Y}$ . We first derive required derivatives of  $w_1$  and  $w_2$ . By the normalization of income, we have

$$w_1(y)x_1(y) + w_2(y)x_2(y) = w_1(y)(\bar{x} + y) + w_2(y)(\bar{x} - y) = 1 \quad \forall y \in \mathcal{Y} \quad (\text{A.48})$$

and  $w_1(0) = w_2(0) = \bar{w} \equiv 1$ . These imply

$$w_1'(0) = -w_2'(0), \quad w_1''(0) = w_2''(0) = -\frac{2}{\bar{x}} w_1'(0), \quad \text{and} \quad w_1'''(0) = -w_2'''(0). \quad (\text{A.49})$$

For instance, we have  $w'_1(y)(\bar{x} + y) + w_1(y) + w'_2(y)(\bar{x} - y) - w'_2(y) = 0$ . With  $w_1(0) = w_2(0) = 1$ , it implies that  $w'_1(0) = -w'_2(0)$ , which is a manifestation that the regions are symmetric when  $y = 0$ .

In fact,  $w'_1(0)$  is the eigenvalue of  $\mathbf{W}_x(\bar{x})$  associated with  $\mathbf{z} = (1, -1)$ , because we have

$$w'_1(0) = \frac{\partial w_1(\bar{x})}{\partial x_1} \frac{\partial x_1(0)}{\partial y} + \frac{\partial w_1(\bar{x})}{\partial x_2} \frac{\partial x_2(0)}{\partial y} = \frac{\partial w_1(\bar{x})}{\partial x_1} - \frac{\partial w_1(\bar{x})}{\partial x_2} \quad (\text{A.50})$$

$$w'_2(0) = \frac{\partial w_2(\bar{x})}{\partial x_1} \frac{\partial x_1(0)}{\partial y} + \frac{\partial w_2(\bar{x})}{\partial x_2} \frac{\partial x_2(0)}{\partial y} = \frac{\partial w_2(\bar{x})}{\partial x_1} - \frac{\partial w_2(\bar{x})}{\partial x_2} = -w'_1(0), \quad (\text{A.51})$$

which is,  $w'_1(0)\mathbf{z} = \mathbf{W}_x(\bar{x})\mathbf{z}$ . Therefore, we have

$$w'_1(0) = -\frac{\bar{w}}{\bar{x}} \cdot \frac{1 - (\sigma - 1)(1 + \chi)\lambda}{\Omega^b(\chi)}, \quad (\text{A.52})$$

where we recall  $\Omega^b(\chi) \equiv \sigma + (\sigma - 1)\chi$ . Then,  $w''(0)$  can be evaluated by the second identity in (A.49). Also, by a patient algebra, we compute  $w'''_1(0)$  as follows:

$$w'''_1(0) = \frac{2}{\bar{x}^3} \left( -3\lambda^2 + \frac{3\lambda(1 + \lambda)(3 + \lambda)}{\Omega^b(\chi)} + \left( -\frac{3(\sigma + 1)}{\Omega^b(\chi)^2} + \frac{2\sigma(\sigma + 1)}{\Omega^b(\chi)^3} - \frac{\sigma(2\sigma - 1)}{\Omega^b(\chi)^4} \right) (1 + \lambda)^3 \right). \quad (\text{A.53})$$

Further,  $\mathbf{a}(y) = (a_1(y), a_2(y)) \equiv (a_1(\mathbf{x}(y)), a_2(\mathbf{x}(y)))$  satisfy

$$\frac{\bar{x}}{a_1(0)} a'_1(0) = -\frac{\bar{x}}{a_2(0)} a'_2(0) = \frac{\bar{x}}{\bar{a}} (1 - \psi) = \frac{1 - \psi}{1 + \psi} = \lambda \quad (\text{A.54})$$

and  $a''_i(0) = a'''_i(0) = \dots = 0$ . We note that  $a_1(0) = a_2(0) = \bar{a} \equiv \bar{x}(1 + \psi)$ .

By direct computations employing the above results, we confirm that

$$\Delta v''(0, \mu^*) = \bar{v}(1 - \chi) \left( -w'_1(0)^2 + w'_2(0)^2 + w''_1(0) - w''_2(0) \right) = 0 \quad (\text{A.55})$$

from (A.49). Therefore, the second condition in (A.41) is met.

After some tedious calculations and manipulations, we get:

$$\Delta v'''(0, \mu^*) = -\frac{4\bar{v}}{\bar{x}^3} \cdot \frac{(1 + \lambda)^3}{\Omega^b(\chi)^4} \cdot \Theta, \quad (\text{A.56})$$

where we define

$$\Theta \equiv \sigma(2\sigma - 1) + \Omega^b(\chi) \left( 3 + \sigma \left( (\sigma + 1)\chi^2 + (4\sigma - 5)\chi + \sigma - 5 \right) \right). \quad (\text{A.57})$$

We can show  $\Theta > 0$  provided that bifurcation occur (i.e., condition (A.44) is satisfied). Since the other components of  $\Delta v'''(0, \mu^*)$  are obviously negative, we have  $\Delta v'''(0, \mu^*) < 0$  at critical values of  $\phi$  or  $\psi$ .

Thus, all the five conditions in (A.41) are met at  $\bar{x}$ . The economy undergoes pitchfork bifurcations along smooth paths where either the freeness of social interactions or the freeness of trade increases, at the break points defined by  $\psi^*$  and  $\phi^*$ , respectively. Moreover,  $\Delta v'''(0, \mu^*) < 0$  implies that the pitchfork bifurcations are supercritical, i.e., the bifurcated branches are stable.  $\square$

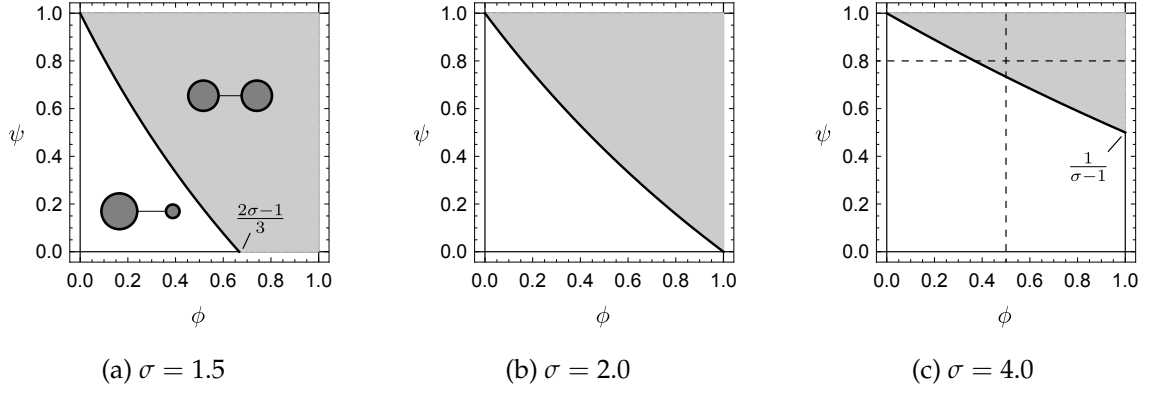


**Figure 11:** Stability of  $\bar{x}$  in the two-region economy.

*Notes:* The uniform distribution  $\bar{x}$  is stable for the shaded (gray) region of  $(\phi, \psi)$  and the black solid curve indicates the critical pair of  $(\phi, \psi)$  where  $\bar{x}$  becomes unstable. The horizontal and vertical dashed lines in Figure 11c correspond to the parametric paths for the bifurcation diagrams Figure 2a and Figure 2b, respectively. The schematic on each (gray or white) parametric region indicates the representative spatial pattern in the parametric region.

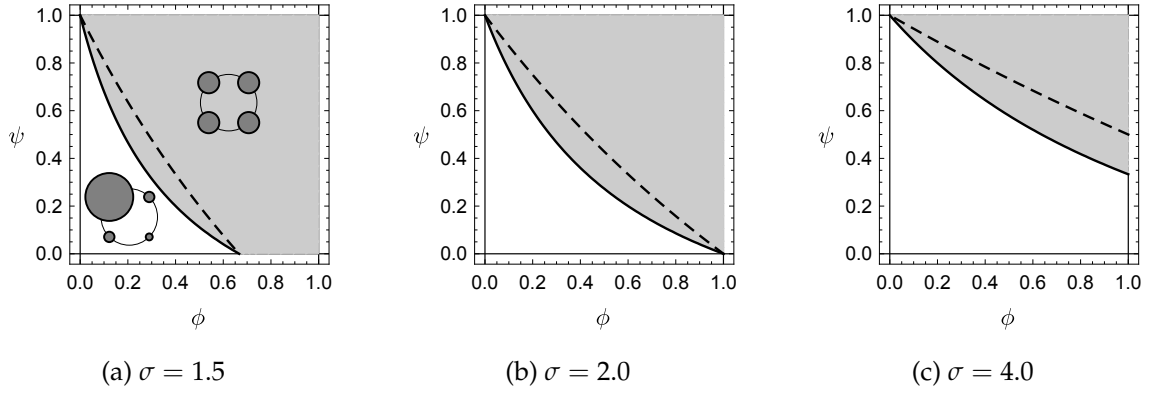


**Figure 12:** Stability of  $\bar{x}$  in the four-region economies with  $\mathbf{G}^{\square}$  and  $\mathbf{G}^{\times} = \mathbf{G}^{\boxtimes}|_{\psi'=\psi}$ .

*Notes:* The black solid curves show the critical pairs  $(\phi^*, \psi^*)$  at which  $\bar{x}$  becomes unstable for the case  $\mathbf{G} = \mathbf{G}^{\boxtimes}$  with  $\psi' = \psi$ . The dashed curves are those for the case  $\mathbf{G} = \mathbf{G}^{\square}$ . The uniform distribution  $\bar{x}$  is stable for the regions above these curves, where the gray regions correspond to  $\mathbf{G} = \mathbf{G}^{\times}$ . Observe that the solid curves always stay below the dashed curves. That is,  $\bar{x}$  is stable for a wider range of  $(\phi, \psi)$  when the economy is more connected.

## B Variations in the elasticity of substitution

Figures 11 and 12 report, respectively, variations of Figures 1 and 8 for three values of  $\sigma$  which are chosen to exhaust all representative forms of the partition of the  $(\phi, \psi)$ -space. For an empirically relevant range of  $\sigma$  (between 3 and 10), the qualitative shape of the partitions stay invariant.

## References

- Ahlfeldt, Gabriel M., Stephen J. Redding, Daniel M. Sturm, and Nikolaus Wolf, "The economics of density: Evidence from the Berlin Wall," *Econometrica*, 2015, 83 (6), 2127–2189.
- Akamatsu, Takashi, Tomoya Mori, Minoru Osawa, and Yuki Takayama, "Endogenous agglomeration in a many-region world," 2019. <https://arxiv.org/abs/1912.05113>.
- , Yuki Takayama, and Kiyohiro Ikeda, "Spatial discounting, Fourier, and racetrack economy: A recipe for the analysis of spatial agglomeration models," *Journal of Economic Dynamics and Control*, 2012, 99 (11), 32–52.
- Allen, Treb, "Modern Spatial Economics (Short Course Lecture Notes)," <https://sites.google.com/site/treballen/graduate-trade> 2019. Online; accessed 24 October 2019.
- and Costas Arkolakis, "Trade and the topography of the spatial economy," *The Quarterly Journal of Economics*, 2014, 129 (3), 1085–1140.
- Alvarez, Fernando and Robert E. Lucas, "General equilibrium analysis of the Eaton–Kortum model of international trade," *Journal of Monetary Economics*, 2007, 54 (6), 1726–1768.
- Anderson, James E. and Eric Van Wincoop, "Trade costs," *Journal of Economic literature*, 2004, 42 (3), 691–751.
- Armington, Paul S., "A theory of demand for product distinguished by place of production," *International Monetary Fund Staff Papers*, 1969, 16 (1), 159–178.
- Baldwin, Richard, *The Great Convergence*, Harvard University Press, 2016.
- Barbero, Javier and José L Zofío, "The multiregional core-periphery model: The role of the spatial topology," *Networks and Spatial Economics*, 2016, 16 (2), 469–496.
- Baum-Snow, Nathaniel, "Did highways cause suburbanization?," *The Quarterly Journal of Economics*, May 2007, 122 (2), 775–805.
- , Loren Brandt, J. Vernon Henderson, Matthew A. Turner, and Qinghua Zhang, "Roads, railroads, and decentralization of Chinese cities," *Review of Economics and Statistics*, 2017, 99 (3), 435–448.
- Beckmann, Martin J., "Spatial equilibrium in the dispersed city," in Yorgos Y. Papageorgiou, ed., *Mathematical Land Use Theory*, Lexington Book, 1976.
- Berliant, Marcus and Masahisa Fujita, "Culture and diversity in knowledge creation," *Regional Science and Urban Economics*, 2012, 42 (4), 648–662.
- Brown, George W. and John von Neumann, "Solutions of games by differential equations," in Harold W. Kuhn and Albert W. Tucker, eds., *Contributions to the Theory of Games I*, Princeton University Press, 1950.
- Dupuis, Paul and Anna Nagurney, "Dynamical systems and variational inequalities," *Annals of Operations Research*, 1993, 44 (1), 7–42.
- Duranton, Gilles and Diego Puga, "Nursery cities: Urban diversity, process innovation, and the life cycle of products," *American Economic Review*, 2001, 91 (5), 1454–1477.
- Facchinei, Francisco and Jong-Shi Pang, *Finite-dimensional Variational Inequalities and Complementarity Problems*, Springer Science & Business Media, 2003.
- Fujita, Masahisa, "Towards the new economic geography in the brain power society," *Regional Science and Urban Economics*, 2007, 37 (4), 482–490.
- and Hideaki Ogawa, "Multiple equilibria and structural transition of non-monocentric urban configurations," *Regional Science and Urban Economics*, 1982, 12, 161–196.
- and Jacques-François Thisse, *Economics of Agglomeration: Cities, Industrial Location, and Regional Growth (2nd Edition)*, Cambridge University Press, 2013.

- **and Tomoya Mori**, “Frontiers of the new economic geography,” *Papers in Regional Science*, 2005, 84 (3), 377–405.
- , **Paul Krugman**, and **Anthony Venables**, *The Spatial Economy: Cities, Regions, and International Trade*, Princeton University Press, 1999.
- Gaspar, José M, Sofia B.S.D. Castro, and João Correia da Silva**, “Agglomeration patterns in a multi-regional economy without income effects,” *Economic Theory*, 2018, 66 (4), 863–899.
- Gaspar, José M., Sofia B.S.D. Castro, and João Correia da Silva**, “The Footloose Entrepreneur model with a finite number of equidistant regions,” *International Journal of Economic Theory*, 2019.
- Helpman, Elhanan**, “The size of regions,” in D. Pines, E. Sadka, and I. Zilcha, eds., *Topics in Public Economics: Theoretical and Applied Analysis*, Cambridge University Press, 1998, pp. 33–54.
- Helsley, Robert W. and William C. Strange**, “Coagglomeration, clusters, and the scale and composition of cities,” *Journal of Political Economy*, 2014, 122 (5), 1064–1093.
- **and Yvess Zenou**, “Social networks and interactions in cities,” *Journal of Economic Theory*, 2014, 150, 426–466.
- Horn, Roger A. and Charles R. Johnson**, *Matrix Analysis*, Cambridge University Press, 2012.
- Ikeda, Kiyohiro, Takashi Akamatsu, and Tatsuhito Kono**, “Spatial period-doubling agglomeration of a core–periphery model with a system of cities,” *Journal of Economic Dynamics and Control*, 2012, 36 (5), 754–778.
- Jackson, Matthew O.**, *Social and Economic Networks*, Princeton University Press, 2010.
- Krugman, Paul R.**, “Increasing returns and economic geography,” *Journal of Political Economy*, 1991, 99 (3), 483–499.
- , “On the number and location of cities,” *European Economic Review*, 1993, 37 (2), 293–298.
- Kuznetsov, Yuri A.**, *Elements of Applied Bifurcation Theory (3rd Eds.)*, Springer-Verlag, 2004.
- Lucas, Robert E. and Esteban Rossi-Hansberg**, “On the internal structure of cities,” *Econometrica*, 2002, 70 (4), 1445–1476.
- Mas-Colell, Andreu, Michael Dennis Whinston, Jerry R. Green et al.**, *Microeconomic Theory*, Vol. 1, Oxford University Press, 1995.
- Matsuyama, Kiminori**, “Geographical advantage: Home market effect in a multi-region world,” *Research in Economics*, 2017, 71 (4), 740–758.
- Nash, John**, “Non-cooperative games,” *Annals of Mathematics*, 1951, 54 (2), 286–295.
- Osawa, Minoru and Takashi Akamatsu**, “Equilibrium refinement for a model of non-monocentric internal S structures of cities: A potential game approach,” *Mimeo*, 2019.
- Ottaviano, Gianmarco I.P. and Giovanni Peri**, “The economic value of cultural diversity: Evidence from US cities,” *Journal of Economic geography*, 2006, 6 (1), 9–44.
- **and** — , “Immigration and national wages: Clarifying the theory and the empirics,” Technical Report, National Bureau of Economic Research 2008.
- **and Giovanni Prarolo**, “Cultural identity and knowledge creation in cosmopolitan cities,” *Journal of Regional Science*, 2009, 49 (4), 647–662.
- Picard, Pierre M. and Yves Zenou**, “Urban spatial structure, employment and social ties,” *Journal of Urban Economics*, 2018, 104, 77–93.
- Rosenthal, Stuart S. and William C. Strange**, “How close is close? The spatial reach of agglomeration economies,” 2019. Unpublished manuscript.

**Sandholm, William H.**, *Population Games and Evolutionary Dynamics*, MIT Press, 2010.

**Smith, Michael J.**, "The stability of a dynamic model of traffic assignment: An application of a method of Lyapunov," *Transportation Science*, 1984, 18 (3), 245–252.

**Tabuchi, Takatoshi**, "Urban agglomeration and dispersion: A synthesis of Alonso and Krugman," *Journal of Urban Economics*, 1998, 44 (3), 333–351.

—, "Historical trends of agglomeration to the capital region and new economic geography," *Regional Science and Urban Economics*, 2014, 44, 50–59.

— **and Jacques-François Thisse**, "A new economic geography model of central places," *Journal of Urban Economics*, 2011, 69 (2), 240–252.

**Taylor, Peter D. and Leo B. Jonker**, "Evolutionarily stable strategies and game dynamics," *Mathematical Biosciences*, 1978, 40, 145–156.

**Wiggins, Stephen**, *Introduction to Applied Nonlinear Dynamical Systems and Chaos*, Springer Science & Business Media, 2003.